CHAPTER 3

COMPUTATIONAL ALGORITHM FOR FINANCIAL MATHEMATICAL MODEL BASED ON EUROPEAN OPTION

In this chapter, we proposed a computational algorithm for the time-fractional Black-Scholes model governing European option. This chapter is organized as follows: In Section 3.2, we discuss the discretization of the time-fractional derivative by L1-2 approximation. Section 3.3 talks about the functional approximation by the operational matrix approach based on the shifted Legendre polynomial (SLP) and shifted Chebyshev polynomial (SCP) as basis function. In Section 3.4, we derive the numerical scheme for TFBSM. Section 3.5 deals with the theoretical stability and convergence of the numerical scheme. In order to show the effectiveness and accuracy of our designed scheme and effect of various parameters on the option pricing, five numerical examples of the TFBSM governing various European options are discussed in Section 3.6. Finally, the conclusion of this chapter is given in Section 3.7.

3.1 Introduction

3.1.1 The time-fractional Black-Scholes model

In this chapter, we consider the following time-fractional Black-Scholes model for pricing European option

$$\frac{\partial^\alpha \mathcal{C}(S,\zeta)}{\partial \zeta^\alpha} + \frac{1}{2}\sigma^2 S^2 \frac{\partial^2 \mathcal{C}(S,\zeta)}{\partial S^2} + rS\frac{\partial \mathcal{C}(S,\zeta)}{\partial S} - r\mathcal{C}(S,\zeta) = 0, (S,\zeta) \in (0,\infty)\times(0,T), \tag{3.1}$$

with the boundary (barrier) conditions

$$\mathcal{C}(0,\zeta) = \mathcal{G}_1(\zeta),\ \mathcal{C}(\infty,\zeta) = \mathcal{G}_2(\zeta), \tag{3.2}$$

and final (terminal) condition

$$\mathcal{C}(S,T) = \mathcal{V}(S). \tag{3.3}$$

Here, $0 < \alpha < 1$, ζ is the current time, S is the stock price, $\mathcal{C}$ is the European option price, T is the maturity date of the contract, r is the risk-free rate, and σ represents the volatility of the returns from the holding stock price S. The fractional derivative in (3.1) is a modified right Riemann-Liouville (RL) derivative which is defined as

$$\frac{\partial^\alpha \mathcal{C}(S,\zeta)}{\partial \zeta^\alpha} = \begin{cases} \dfrac{1}{\Gamma(1-\alpha)}\dfrac{d}{d\zeta}\displaystyle\int_\zeta^T \frac{\mathcal{C}(S,\xi)-\mathcal{C}(S,T)}{(\xi-\zeta)^\alpha}d\xi, & 0<\alpha<1, \\ \dfrac{\partial \mathcal{C}(S,\zeta)}{\partial \zeta}, & \alpha = 1. \end{cases} \tag{3.4}$$

Let $\zeta = T - t$, then

$$\begin{aligned}\frac{\partial^\alpha \mathcal{C}(S,\zeta)}{\partial \zeta^\alpha} &= \frac{1}{\Gamma(1-\alpha)}\frac{d}{d\zeta}\int_{\zeta}^{T}\frac{\mathcal{C}(S,\xi)-\mathcal{C}(S,T)}{(\xi-\zeta)^\alpha}d\xi,\\ &= \frac{1}{\Gamma(1-\alpha)}\frac{-d}{dt}\int_{T-t}^{T}\frac{\mathcal{C}(S,\xi)-\mathcal{C}(S,T)}{(\xi-(T-t))^\alpha}d\xi,\\ &= \frac{-1}{\Gamma(1-\alpha)}\frac{d}{dt}\int_{0}^{t}\frac{\mathcal{C}(S,T-\eta)-\mathcal{C}(S,T)}{(t-\eta)^\alpha}d\eta. \qquad (3.5)\end{aligned}$$

Suppose, $x = \ln S$ and $\mathcal{U}(x,t) = \mathcal{C}(e^x, T-t)$ then

$${}_0^{RL}D_t^\alpha \mathcal{U}(x,t) = \frac{1}{2}\sigma^2\frac{\partial^2\mathcal{U}(x,t)}{\partial x^2} + (r-\frac{\sigma^2}{2})\frac{\partial \mathcal{U}(x,t)}{\partial x} - r\mathcal{U}(x,t), (x,t) \in \mathbb{R}\times(0,T), \qquad (3.6)$$

with boundary and initial conditions

$$\mathcal{U}(-\infty,t) = \mathcal{G}_1(t),\ C(\infty,t) = \mathcal{G}_2(t), \qquad (3.7)$$

$$\mathcal{U}(x,0) = \mathcal{H}(x). \qquad (3.8)$$

where ${}_0^{RL}D_t^{\alpha}\mathcal{U}(x,t)$ is the modified left RL derivative of order α $(0<\alpha<1)$ which is defined as

$$\begin{aligned}
{}_0^{RL}D_t^{\alpha}\mathcal{U}(x,t) &= \frac{1}{\Gamma(1-\alpha)}\frac{d}{dt}\int_0^t \frac{\mathcal{U}(x,\eta)-\mathcal{U}(x,0)}{(t-\eta)^{\alpha}}d\eta,\\
&= \frac{1}{\Gamma(1-\alpha)}\frac{d}{dt}\int_0^t \frac{\mathcal{U}(x,\eta)}{(t-\eta)^{\alpha}}d\eta - \frac{1}{\Gamma(1-\alpha)}\frac{d}{dt}\int_0^t \frac{\mathcal{U}(x,0)}{(t-\eta)^{\alpha}}d\eta\\
&= \frac{\mathcal{U}(x,0)t^{-\alpha}}{\Gamma(1-\alpha)} + \frac{1}{\Gamma(1-\alpha)}\int_0^t \frac{\mathcal{U}'(x,\eta)}{(t-\eta)^{\alpha}}d\eta - \frac{\mathcal{U}(x,0)t^{-\alpha}}{\Gamma(1-\alpha)}\\
&= \frac{1}{\Gamma(1-\alpha)}\int_0^t \frac{\mathcal{U}'(x,\eta)}{(t-\eta)^{\alpha}}d\eta\\
&= {}_0^{C}D_t^{\alpha}\mathcal{U}(x,t). \qquad (3.9)
\end{aligned}$$

where ${}_0^{C}D_t^{\alpha}\mathcal{U}(x,t)$ is the Caputo derivative of order α. Now, in order to solve the TFBSM (3.6)-(3.8) numerically, we will truncate the infinte domain $\mathbb{R}\times(0,T)$ into a finite domain $(x_L,x_R)\times(0,T)$. Thus, the TFBSM becomes

$${}_0^{C}D_t^{\alpha}\mathcal{U}(x,t) = a\frac{\partial^2\mathcal{U}(x,t)}{\partial x^2} + b\frac{\partial\mathcal{U}(x,t)}{\partial x} - c\mathcal{U}(x,t) + f(x,t), (x,t)\in(x_L,x_R)\times(0,T), \qquad (3.10)$$

with boundary and initial conditions

$$\mathcal{U}(x_L,t) = \mathcal{G}_1(t),\ \mathcal{U}(x_R,t) = \mathcal{G}_2(t) \qquad (3.11)$$

$$\mathcal{U}(x,0) = \mathcal{H}(x). \qquad (3.12)$$

where, $a=\frac{1}{2}\sigma^2>0$, $b=r-a$, $c=r>0$. Here, the source function $f(x,t)$ is used for the purpose of validation.

- If $a > 0,\ b < 0$ and $c = 0$, then the Eq. (3.10) reduces to time-fractional advection diffusion equation (TFADE).
- If $a > 0,\ b = 0$ and $c = 0$, then the Eq. (3.10) reduces to time-fractional diffusion equation (TFDE).
- If $a > 0,\ b = 0$ and $c \neq 0$, then the Eq. (3.10) reduces to time-fractional reaction-diffusion equation (TFRDE).

3.1.2 Main contribution of this chapter

The operational matrix approach is also considered to be an effective and highly accurate method for solving the fractional PDEs [53, 168–171]. Therefore, the present chapter is mainly focused on designing a high order and highly accurate, stable computational approach based on the combination of finite difference method with operational matrix approach to solve the TFBSM and to study the role of various parameters on the European option pricing. The contributions of the chapter are described in the following points:

- We have applied the L1-2 approximation for discretizing the time-fractional derivative and meshfree operational matrix approach based on SLP and SCP basis function in the spatial direction. The L1-2 approximation first converts the TFBSM into a system of ordinary differential equations (ODE) in space variables at each time level. Then, the operational matrix transforms the system of ODE's into a system of linear algebraic equations which are easy to solve.

- We have established a new relation between $c_1^{(\alpha)}$ and $c_2^{(\alpha)}$ which was not discussed earlier by [102]. This helps us to prove the theoretical unconditional stability and convergence analysis of the numerical scheme for $\alpha \in (0, \bar{\alpha}]$.

- Stability of the numerical scheme is also verified numerically for all α, by adding some noise in the initial data.

- The proposed numerical scheme has been tested on five test models and it is observed that with this computational approach, the accuracy is almost the same with respect to both the basis functions but the CPU time taken by scheme with SLP basis is less than the SCP basis function.

- A comparative study of the numerical results by our proposed scheme with the existing schemes given by [1] and [2] have been discussed. It reflects that the proposed scheme is more error efficient and reliable than earlier schemes.

- A study on the effects of different parameters such as fractional order, volatility, interest rate, and strike price on the European call and put option pricing have been analyzed.

To our knowledge, this approach is new and has not been reported so far to solve TFBSM.

3.2 Temporal discretization

3.2.1 L1-2 approximation of the Caputo derivatives

Let $\{t_k = k\tau,\ k = 0, 1, 2, ..., N;\ T = \tau N\}$ be node points and N be the the number of grid point in time direction. Suppose $\mathcal{U}(t) \in C^3[0, t_k]$, $k \geq 0$. From the definition

of Caputo derivatives for any $\alpha \in (0,1)$ at any point t_k is given by

$$ {}_0^C D_t^\alpha \mathcal{U}(t)|_{t=t_k} = \frac{1}{\Gamma(1-\alpha)} \int_0^{t_k} \frac{\mathcal{U}'(s)}{(t_k - s)^\alpha} ds, \tag{3.13} $$

Let ${}_0\mathbb{D}_t^\alpha \mathcal{U}(t)$ be the L1-2 approximation [102] of the Caputo fractional derivatives ${}_0^C D_t^\alpha \mathcal{U}(t)$,

$$ {}_0\mathbb{D}_t^\alpha \mathcal{U}(t)|_{t=t_k} = \frac{\tau^{1-\alpha}}{\Gamma(2-\alpha)} \sum_{j=1}^{k} c_{k-j}^{(\alpha)} \delta_t \mathcal{U}_{j-\frac{1}{2}}, \tag{3.14} $$

$$ = \frac{\tau^{-\alpha}}{\Gamma(2-\alpha)} \left[c_0^{(\alpha)} \mathcal{U}(t_k) - \sum_{j=1}^{k-1} \left(c_{k-j-1}^{(\alpha)} - c_{k-j}^{(\alpha)} \right) \mathcal{U}(t_j) - c_{k-1}^{\alpha} \mathcal{U}(t_0) \right], \tag{3.15} $$

where, $c_0^{(\alpha)} = a_0^{(\alpha)} = 1$ for $k = 1$. For $k \geq 2$,

$$ c_j^{(\alpha)} = \begin{cases} a_0^{(\alpha)} + b_0^{(\alpha)}, & j = 0, \\ a_j^{(\alpha)} + b_j^{(\alpha)} - b_{j-1}^{(\alpha)}, & 1 \leq j \leq k-2, \\ a_j^{(\alpha)} - b_{j-1}^{(\alpha)}, & j = k-1. \end{cases} \tag{3.16} $$

where, $a_j^{(\alpha)}$ and $b_j^{(\alpha)}$ is given below. where,

$$ \begin{aligned} a_j^{(\alpha)} &= (j+1)^{1-\alpha} - j^{1-\alpha} \qquad\qquad 0 \leq j \leq k-1, \\ b_j^{(\alpha)} &= \frac{1}{(2-\alpha)} \left[(j+1)^{2-\alpha} - j^{2-\alpha} \right] - 0.5 \left[(j+1)^{1-\alpha} + j^{1-\alpha} \right], \ j \geq 0. \end{aligned} \tag{3.17} $$

Let, the truncation term in L1-2 approximation (3.15) is defined as

$$ r_\tau^k = {}_0^C D_t^\alpha \mathcal{U}(t)|_{t=t_k} - {}_0\mathbb{D}_t^\alpha \mathcal{U}(t)|_{t=t_k}. \tag{3.18} $$

Therefore, the equivalent form of TFBSM (3.10)-(3.12) is

$$ {}_0\mathbb{D}_t^{\alpha}\mathcal{U}(t_k) - a\frac{\partial^2\mathcal{U}(t_k)}{\partial x^2} - b\frac{\partial\mathcal{U}(t_k)}{\partial x} + c\mathcal{U}(t_k) = f(t_k) - r_{\tau}^{k}, \tag{3.19} $$

The above reformulation motivates the following time scheme

$$ {}_0\mathbb{D}_t^{\alpha}\mathcal{U}^{k} - a\frac{\partial^2\mathcal{U}^{k}}{\partial x^2} - b\frac{\partial\mathcal{U}^{k}}{\partial x} + c\mathcal{U}^{k} = f^{k}. \tag{3.20} $$

where, $\mathcal{U}^k$ is an approximation of $\mathcal{U}(t_k)$. The truncation term r_τ^k is an indicator of how accurate an approximation is, which is estimated in Theorem 3.3.

Remark 3.1. [102] did not discuss about the relation between $c_1^{(\alpha)}$ and $c_2^{(\alpha)}$ which plays an important role in the stability analysis. We investigated this relationship and will further use it in proving the stability and convergence of the numerical scheme.

Lemma 3.2. If $0 < \alpha \leq \bar{\alpha}$, $c_1^{(\alpha)} \geq c_2^{(\alpha)}$ and if $\alpha \in (\bar{\alpha},1)$, $c_1^{(\alpha)} < c_2^{(\alpha)}$. Therefore $c_0^{(\alpha)} \geq c_1^{(\alpha)} \geq c_2^{(\alpha)} \geq \cdots \geq c_{k-1}^{(\alpha)}$ when $0 < \alpha \leq \bar{\alpha}$, where $\bar{\alpha} = 0.3739$.

Proof. By the definition of $c_j^{(\alpha)}$ for $(0 \geq j \geq k-1, k \geq 3)$ when $(0 < \alpha < 1)$,
$c_0^{(\alpha)} = a_0^{(\alpha)} + b_0^{(\alpha)} = \dfrac{1}{2} + \dfrac{1}{2-\alpha} \in (1, 1.5)$,
$c_1^{(\alpha)} = a_1^{(\alpha)} + b_1^{(\alpha)} - b_0^{\alpha} = (2^{-\alpha} - 1) + \dfrac{1}{(2-\alpha)}(2^{2-\alpha} - 2) \in (-0.5, 1)$.
In fact $c_1^{(\alpha)} > 0$ for $0 < \alpha < 0.68029$ and $c_1^{(\alpha)} < 0$ for $0.680290 < \alpha < 1$.

Now, for $2 \leq j \leq k-2$, $c_j^{(\alpha)} = a_j^{(\alpha)} + b_j^{(\alpha)} - b_{j-1}^{(\alpha)}$.

therefore,

$$ \begin{aligned} c_2^{(\alpha)} &= a_2^{(\alpha)} + b_2^{(\alpha)} - b_1^{(\alpha)}, \\ &= (3^{1-\alpha} - 2^{1-\alpha}) + \frac{1}{2-\alpha}(3^{2-\alpha} - 2.2^{2-\alpha} + 1) - \frac{1}{2}(3^{1-\alpha} - 1) \in (0, 1). \end{aligned} \tag{3.21} $$

Now,

$$c_1^{(\alpha)} - c_2^{(\alpha)} = \frac{1}{2-\alpha}(3.2^{2-\alpha} - 3^{2-\alpha} - 3) - \frac{1}{2}(3.2^{1-\alpha} - 3^{1-\alpha} - 3). \tag{3.22}$$

Let $\phi(x) = \frac{1}{2-x}(3.2^{2-x} - 3^{2-x} - 3) - \frac{1}{2}(3.2^{1-x} - 3^{1-x} - 3)$, then the only zeros of $\phi(x)$ in $(0,1)$ can be found at $x = 0.3739$. It has been observed that $\phi(x) > 0$ when $x \in (0, 0.3739)$ and $\phi(x) < 0$ when $x \in (0.3739, 1)$.

Thus, $c_1^{(\alpha)} - c_2^{(\alpha)} \geq 0$ when $0 < \alpha \leq 0.3739$ and $c_1^{(\alpha)} - c_2^{(\alpha)} < 0$ when $\alpha \in (0.3739, 1)$. Since ,we know that $c_2^{(\alpha)} \geq c_3^{(\alpha)} \geq \cdots \geq c_{k-1}^{(\alpha)}$ for $k \geq 3$, hence, we can write $c_0^{(\alpha)} \geq c_1^{(\alpha)} \geq c_2^{(\alpha)} \geq \cdots \geq c_{k-1}^{(\alpha)}$ when $0 < \alpha \leq 0.3739$. □

Theorem 3.3. *Suppose $\mathcal{U}(t) \in C^3[0, t_k]$. For any α $(0 < \alpha < 1)$, let the truncation term is*

$$r_\tau^k = R(\mathcal{U}(t_k)) = {}_0^C D_t^\alpha \mathcal{U}(t)|_{t=t_k} - {}_0\mathbb{D}_t^\alpha \mathcal{U}(t)|_{t=t_k}. \tag{3.23}$$

Then we have,

1. $|r_\tau^1| = |R(\mathcal{U}(t_1))| \leq C_\alpha M(\mathcal{U})\tau^{2-\alpha}$**,**

2. $|r_\tau^k| = |R(\mathcal{U}(t_k))| \leq C_\alpha M(\mathcal{U})\tau^{2-\alpha} + \tilde{C}_\alpha \tilde{M}(\mathcal{U})\tau^{3-\alpha}$**,** $k \geq 2$**.**

where, $C_\alpha = \frac{\alpha}{2\Gamma(3-\alpha)}$, $\tilde{C}_\alpha = \left[\frac{1}{12\Gamma(1-\alpha)} + \frac{\alpha(5-\alpha)}{6\Gamma(4-\alpha)}\right]$,

$M(\mathcal{U}) = \max_{t_0 \leq t \leq t_1} |\mathcal{U}''(t)|$, $\tilde{M}(\mathcal{U}) = \max_{t_0 \leq t \leq t_k} |\mathcal{U}'''(t)|$.

Proof. From Theorem 2.1 of [102], for $k \geq 2$, we have

$$|R(\mathcal{U}(t_k))| \leq \frac{1}{\Gamma(1-\alpha)} \Bigg\{ \frac{\alpha}{12} \max_{t_0 \leq t \leq t_1} |\mathcal{U}''(t)|(t_k - t_1)^{-\alpha-1}\tau^3 + \left[\frac{1}{12} + \frac{\alpha}{3(1-\alpha)(2-\alpha)}\left(\frac{1}{2} + \frac{1}{3-\alpha}\right)\right] \max_{t_0 \leq t \leq t_k} |\mathcal{U}'''(t)|\tau^{3-\alpha} \Bigg\}, \tag{3.24}$$

$$|R(\mathcal{U}(t_k))| \leq \frac{\alpha}{12\Gamma(1-\alpha)} \max_{t_0 \leq t \leq t_1} |\mathcal{U}''(t)|((k-1)\tau)^{-\alpha-1}\tau^3 + \left[\frac{1}{12\Gamma(1-\alpha)} + \frac{\alpha(5-\alpha)}{6\Gamma(4-\alpha)}\right] \max_{t_0 \leq t \leq t_k} |\mathcal{U}'''(t)|\tau^{3-\alpha}. \tag{3.25}$$

Since $\dfrac{\alpha}{12\Gamma(1-\alpha)} \dfrac{1}{(k-1)^{\alpha+1}} \leq \dfrac{\alpha}{2\Gamma(3-\alpha)}$ for all $\alpha \in (0,1)$. Therefore,

$$|r_\tau^k| = |R(\mathcal{U}(t_k))| \leq C_\alpha M(\mathcal{U})\tau^{2-\alpha} + \tilde{C}_\alpha \tilde{M}(\mathcal{U})\tau^{3-\alpha}, \tag{3.26}$$

where, $C_\alpha = \dfrac{\alpha}{2\Gamma(3-\alpha)}$, $\tilde{C}_\alpha = \left[\dfrac{1}{12\Gamma(1-\alpha)} + \dfrac{\alpha(5-\alpha)}{6\Gamma(4-\alpha)}\right]$, $M(\mathcal{U}) = \max_{t_0 \leq t \leq t_1} |\mathcal{U}''(t)|$, $\tilde{M}(\mathcal{U}) = \max_{t_0 \leq t \leq t_k} |\mathcal{U}'''(t)|$.

Moreover, from the graphical representation, for $0 < \alpha < 1$, the function C_α is monotonically increasing and $0 < C_\alpha < \dfrac{1}{2}$. Similarly, the function $\tilde{C}_\alpha$ is also monotonically increasing and $\dfrac{1}{12} < \tilde{C}_\alpha < \dfrac{1}{3}$. □

Lemma 3.4. Let $E_\alpha = \Gamma(2-\alpha)C_\alpha$ and $\tilde{E}_\alpha = \Gamma(2-\alpha)\tilde{C}_\alpha$ then for any α $(0 < \alpha < 1)$, it holds

(1) $0 < E_\alpha < C_\alpha < \dfrac{1}{2}$;

(2) $\dfrac{1}{12} < \tilde{E}_\alpha < \tilde{C}_\alpha < \dfrac{1}{3}$.

Proof. Since, by the property of Gamma function, $0 < \Gamma(2-\alpha) < 1$ for $0 < \alpha < 1$, and C_α is monotonically increasing, therefore

(1) $E_\alpha = \Gamma(2-\alpha)C_\alpha < C_\alpha$ and $E_\alpha > 0$. Hence (1) holds.

(2) $\tilde{E}_\alpha = \Gamma(2-\alpha)\tilde{C}_\alpha < \tilde{C}_\alpha$.

$$\tilde{E}_\alpha = \Gamma(2-\alpha)\left[\frac{1}{12\Gamma(1-\alpha)} + \frac{\alpha(5-\alpha)}{6\Gamma(4-\alpha)}\right] \tag{3.27}$$

$$= \left[\frac{(1-\alpha)}{12} + \frac{\alpha(5-\alpha)}{6(2-\alpha)(3-\alpha)}\right] \tag{3.28}$$

Let $\phi(x) = \dfrac{1-x}{12} + \dfrac{x(5-x)}{6(2-x)(3-x)}$,
then $\phi'(x) = -\dfrac{1}{12} + \dfrac{(5-2x)}{(x^2-5x+6)^2} > 0$ for $0 < \alpha < 1$.
Therefore, $\phi(x)$ is monotonically increasing in (0,1) and when $x \to 0$, $\phi(x) \to \dfrac{1}{12}$.
Thus $\dfrac{1}{12} < \tilde{E}_\alpha < \tilde{C}_\alpha < \dfrac{1}{3}$. □

3.3 Basis function and operational matrices

3.3.1 Shifted Legendre polynomials

Let $P_i(x)$ be the Legendre polynomial of order i which is defined over the interval $[-1, 1]$. It satisfies the recursive formula

$$P_{i+1}(x) = \left(\frac{2i+1}{i+1}\right) xP_i(x) - \left(\frac{i}{i+1}\right) P_{i-1}(x), \quad i = 1, 2, 3, ..., \tag{3.29}$$

where, $P_0(x) = 1$, $P_1(x) = x$, $P_2(x) = \dfrac{1}{2}(3x^2 - 1)$,...

The shifted Legendre polynomial defined over the domain $[0, 1]$ is given by

$$p_i(x) = P_i(2x-1), \quad i = 0, 1, 2, 3, ..., \tag{3.30}$$

The Legendre polynomial are orthogonal w.r.t. the weight function $w(x) = 1$ such that

$$\int_0^1 w(x)P_i(x)P_j(x)dx = \begin{cases} \frac{1}{2i+1}\delta_{ij} & \text{for } i = j, \\ 0 & \text{otherwise.} \end{cases} . \tag{3.31}$$

Therefore, the orthonormal shifted Legendre polynomial in [0, 1] is given by

$$\psi_i(x) = \sqrt{i + \frac{1}{2}}P_i(2x - 1), \quad i = 0, 1, 2, 3, \ldots . \tag{3.32}$$

The set $\Psi(x) = [\psi_0(x), \psi_1(x), \ldots, \psi_n(x)]$ form an orthonormal basis of $L_2[0, 1]$ for the polynomial of degree $\leq n$. The orthonormal nature of the SLP saves the computational time in unknown Legendre's coefficient calculation.

3.3.2 Shifted Chebyshev polynomial of second kind

The shifted Chebyshev polynomials of second kind on $[0, 1]$ are given by

$$\phi_i(x) = U_i(2x - 1), \quad i = 0, 1, 2, 3, ... \tag{3.33}$$

where $U_i(x)$ are the Chebyshev polynomials of second kind of order i defined on the interval $[-1, 1]$ and satisfy the following recursive formula.

$$U_{i+1}(x) = 2xU_i(x) - U_{i-1}(x), \quad i = 1, 2, 3, ... \tag{3.34}$$

where $U_0(x) = 1$, $U_1(x) = x$, $U_2(x) = 4x^2 - 1$ and so on. The shifted Chebyshev polynomials of second kind are orthogonal with respect to the weight function

$w(x) = \sqrt{x - x^2}$ such that

$$\int_0^1 w(x)\phi_i(x)\phi_j(x)dx = \begin{cases} \pi/8 & \text{for } i = j, \\ 0 & \text{otherwise.} \end{cases} \tag{3.35}$$

3.3.3 Function approximation

Let $f(x) \in L_2[0,1]$ and $\Psi(x) = [\psi_0(x), \psi_1(x), ..., \psi_M(x)]^T$ be the orthonormal basis of $L_2[0,1]$ then the approximation of the function $f(x)$ can be written as

$$f(x) \approx \sum_{i=0}^{M} f_i\psi_i(x) = F^T\Psi(x), \tag{3.36}$$

where $F = [f_0, f_1, ..., f_M]^T$, and the unknown coefficients f_i are calculated by

$$f_i = \langle f(x), \psi_i(x)\rangle = \int_0^1 w(x)f(x)\psi_i(x)dx. \tag{3.37}$$

3.3.4 The operational matrix

Let $\Psi(x)$ be the orthonormal basis of $L_2[0,1]$ defined in Section 3.3.1, then

$$\int_{x_L}^{x} \Psi(\xi)d\xi = \begin{bmatrix} \int_{x_L}^{x} \psi_0(\xi)d\xi \\ \int_{x_L}^{x} \psi_1(\xi)d\xi \\ \vdots \\ \int_{x_L}^{x} \psi_M(\xi)d\xi \end{bmatrix} = \begin{bmatrix} k_0(x) \\ k_1(x) \\ \vdots \\ k_M(x) \end{bmatrix}. \tag{3.38}$$

Now, approximating $k_i(x)$ as mentioned in (3.36)

$$\begin{bmatrix} k_0(x) \\ k_1(x) \\ \vdots \\ k_M(x) \end{bmatrix} \approx \begin{bmatrix} \sum_{j=0}^{M} k_{0j}\psi_j(x) \\ \sum_{j=0}^{M} k_{1j}\psi_j(x) \\ \vdots \\ \sum_{j=0}^{M} k_{Mj}\psi_j(x) \end{bmatrix} = \begin{bmatrix} k_{00} & k_{01} & \cdots & k_{0M} \\ k_{10} & k_{11} & \cdots & k_{1M} \\ \vdots & & & \\ k_{M0} & k_{M1} & \cdots & k_{MM} \end{bmatrix} \begin{bmatrix} \psi_0(x) \\ \psi_1(x) \\ \vdots \\ \psi_M(x) \end{bmatrix} = K\Psi(x), \tag{3.39}$$

therefore,

$$\int_{x_L}^{x} \Psi(\xi)d\xi = K\Psi(x), \tag{3.40}$$

where,

$$K = \begin{bmatrix} k_{00} & k_{01} & \cdots & k_{0M} \\ k_{10} & k_{11} & \cdots & k_{1M} \\ \vdots & & & \\ k_{M0} & k_{M1} & \cdots & k_{MM} \end{bmatrix} \tag{3.41}$$

is called the operational matrix of integration. The order of K is $(M+1)$. The coefficient k_{ij} can be calculated by

$$k_{ij} = \langle k_i(x), \psi_j(x) \rangle = \int_0^1 w(x)k_i(x)\psi_j(x)dx. \tag{3.42}$$

3.3.5 Spatial approximation

Let $\mathcal{U}^k(x) = \mathcal{U}(x, t_k)$ be the numerical solution of the TFBSM (3.10) at time level t_k for $k = 1, 2, ..., N$ and we want to approximate this solution $\mathcal{U}(x, t_k)$ at each t_k.

To do this, let us suppose

$$\frac{d^2\mathcal{U}^k(x)}{dx^2} \approx \sum_{i=0}^{M} a_i^k \psi_i(x) = A_k^T \Psi(x), \quad k = 1, 2, ..., N, \quad i = 0, 1, ..., M. \tag{3.43}$$

Integrating (3.43) from x_L to x, we get,

$$\int_{x_L}^{x} \frac{d^2\mathcal{U}^k(x)}{dx^2} dx \approx \int_{x_L}^{x} A_k^T \Psi(x) dx,$$

$$\frac{d\mathcal{U}^k(x)}{dx} \approx \frac{d\mathcal{U}^k(x_L)}{dx} + A_k^T \int_{x_L}^{x} \Psi(x) dx, \tag{3.44}$$

again integrating (3.44) from x_L to x, one can obtain

$$\mathcal{U}^k(x) \approx \mathcal{U}^k(x_L) + (x - x_L)\frac{d\mathcal{U}^k(x_L)}{dx} + A_k^T \int_{x_L}^{x}\int_{x_L}^{x} \Psi(x) dx. \tag{3.45}$$

Putting $x = x_R$ and using the boundary condition $u(x_R, t_k) = \mathcal{G}_2(t_k)$ in (3.45), we get

$$\frac{d\mathcal{U}^k(x_L)}{dx} \approx \frac{1}{(x_R - x_L)} \left(\mathcal{G}_2(t_k) - \mathcal{G}_1(t_k) - A_k^T \int_{x_L}^{x_R}\int_{x_L}^{x} \Psi(x) dx \right). \tag{3.46}$$

Using (3.46) in (3.44), we get

$$\frac{d\mathcal{U}^k(x)}{dx} \approx \frac{1}{(x_R - x_L)} \left(\mathcal{G}_2(t_k) - \mathcal{G}_1(t_k) - A_k^T \int_{x_L}^{x_R}\int_{x_L}^{x} \Psi(x) dx \right) + A_k^T \int_{x_L}^{x} \Psi(x) dx,$$

$$\approx \left(G_k^T + A_k^T K_{12} \right) \Psi(x), \tag{3.47}$$

where, $K_{12} = K_1 - K_2$. The calculation of G_k^T, K_1 and K_2 is given in the remark (3.5) and (3.7). Now, using (3.46) in (3.45) and simplifying, we get

$$\begin{aligned}\mathcal{U}^k(x) &\approx \mathcal{G}_1(t_k) + \frac{(x - x_L)}{(x_R - x_L)} \left(\mathcal{G}_2(t_k) - \mathcal{G}_1(t_k) - A_k^T \int_{x_L}^{x_R} \int_{x_L}^{x} \Psi(x) dx \right) + A_k^T \int_{x_L}^{x} \int_{x_L}^{x} \Psi(x) dx, \\ &\approx \left(B_k^T + A_k^T K_{13} \right) \Psi(x), \end{aligned} \tag{3.48}$$

where, $K_{13} = K_1^2 - K_3$. The calculation of B_k^T, K_1^2 and K_3 is given in the remark (3.5) and (3.7).

Remark 3.5. Since $\mathcal{G}_1(t_k)$, $\mathcal{G}_2(t_k)$ are the boundary condition at each time level t_k and are the function of x also therefore assuming

$$\frac{1}{x_R - x_L}(\mathcal{G}_2(t_k) - \mathcal{G}_1(t_k)) = \mathrm{g}(x) \approx G_k^T \Psi(x), \tag{3.49}$$

$$\left(1 - \frac{(x - x_L)}{(x_R - x_L)} \right) \mathcal{G}_1(t_k) + \frac{(x - x_L)}{(x_R - x_L)} \mathcal{G}_2(t_k) = \mathrm{b}(x) \approx B_k^T \Psi(x). \tag{3.50}$$

Remark 3.6. We can approximate the source function $f(x, t_k) \approx F_k^T \Psi(x)$ at each time level t_k and initial condition $\mathcal{U}(x, 0) = \mathcal{H}(x) \approx H^T \Psi(x)$.

Remark 3.7. The operational matrix of integration K_1, K_2 and K_3 are calculated as

$$\int_{x_L}^{x} \Psi(x)dx = \mathrm{k}_1(x) \approx K_1\Psi(x), \tag{3.51}$$

$$\int_{x_L}^{x}\int_{x_L}^{x} \Psi(x)dx = \mathrm{k}_{12}(x) \approx K_1^2\Psi(x), \tag{3.52}$$

$$\frac{1}{(x_R - x_L)}\int_{x_L}^{x_R}\int_{x_L}^{x} \Psi(x)dx = \mathrm{k}_2(x) \approx K_2\Psi(x), \tag{3.53}$$

$$\frac{(x - x_L)}{(x_R - x_L)}\int_{x_L}^{x_R}\int_{x_L}^{x} \Psi(x)dx = \mathrm{k}_3(x) \approx K_3\Psi(x). \tag{3.54}$$

3.4 Derivation of numerical algorithm for TFBSM

In this section, we design the numerical algorithm by combining the finite difference method with operational matrix approach for the TFBSM (3.10)-(3.12). The TFBSM at each time level t_k can be written as

$${}_0^C D_t^{\alpha}\mathcal{U}(x,t_k) = a\frac{\partial^2\mathcal{U}(x,t_k)}{\partial x^2} + b\frac{\partial\mathcal{U}(x,t_k)}{\partial x} - c\mathcal{U}(x,t_k) + f(x,t_k), \tag{3.55}$$

with boundary and initial condition

$$\mathcal{U}(x_L,t_k) = \mathcal{G}_1(t_k),\ \mathcal{U}(x_R,t_k) = \mathcal{G}_2(t_k), \tag{3.56}$$

$$\mathcal{U}(x,0) = \mathcal{H}(x). \tag{3.57}$$

Applying L1-2 approximation of the Caputo derivative at time t_k, $(k \geq 1)$in (3.55) and re-arranging the terms, we have

$$a\frac{\partial^2 \mathcal{U}^k(x)}{\partial x^2} + b\frac{\partial \mathcal{U}^k(x)}{\partial x} - c\mathcal{U}^k(x) = {}_0\mathbb{D}_t^{\alpha}\mathcal{U}^k(x) - f^k(x). \tag{3.58}$$

Since, from (3.15)

$${}_0\mathbb{D}_t^{\alpha}\mathcal{U}^k(x) = \frac{\tau^{-\alpha}}{\Gamma(2-\alpha)}\left[c_0^{(\alpha)}\mathcal{U}^k(x) + \sum_{j=1}^{k-1}\left(c_{k-j}^{(\alpha)} - c_{k-j-1}^{(\alpha)}\right)\mathcal{U}^k(x) - c_{k-1}^{(\alpha)}\mathcal{U}^0(x)\right].$$

Therefore, (3.58) becomes

$$\begin{aligned} a\frac{\partial^2 \mathcal{U}^k(x)}{\partial x^2} + b\frac{\partial \mathcal{U}^k(x)}{\partial x} - c\mathcal{U}^k(x) = dc_0^{(\alpha)}\mathcal{U}^k(x) + d\sum_{j=1}^{k-1}\left(c_{k-j}^{(\alpha)} - c_{k-j-1}^{(\alpha)}\right)\mathcal{U}^k(x) \\ - dc_{k-1}^{(\alpha)}\mathcal{U}^0(x) - f^k(x), \end{aligned} \tag{3.59}$$

where, $d = \dfrac{\tau^{-\alpha}}{\Gamma(2-\alpha)}$.

$$a\frac{\partial^2 \mathcal{U}^k(x)}{\partial x^2} + b\frac{\partial \mathcal{U}^k(x)}{\partial x} - \left(c + dc_0^{(\alpha)}\right)\mathcal{U}^k(x) = d\sum_{j=1}^{k-1}\left(c_{k-j}^{(\alpha)} - c_{k-j-1}^{(\alpha)}\right)\mathcal{U}^k(x) - dc_{k-1}^{(\alpha)}\mathcal{U}^0(x) - f^k(x). \tag{3.60}$$

Now, using the approximation as discussed in Section 3.3.5 in (3.60), we get

$$\begin{aligned} aA_k^T\Psi(x) + b\left(G_k^T + A_k^T K_{12}\right)\Psi(x) - \left(c + dc_0^{(\alpha)}\right)\left(B_k^T + A_k^T K_{13}\right)\Psi(x) \\ = d\sum_{j=1}^{k-1}\left(c_{k-j}^{(\alpha)} - c_{k-j-1}^{(\alpha)}\right)\left(B_k^T + A_k^T K_{13}\right)\Psi(x) - dc_{k-1}^{(\alpha)}H^T\Psi(x) - F_k^T\Psi(x). \end{aligned}$$

Comparing the coefficients of unknowns a_{ij} from both sides, we get $(M+1)$ system of equations at each time level t_k, $(k \geq 1)$.

$$aA_k^T + bA_k^T K_{12} - \left(c + dc_0^{(\alpha)}\right) A_k^T K_{13} = d\sum_{j=1}^{k-1} \left(c_{k-j}^{(\alpha)} - c_{k-j-1}^{(\alpha)}\right) \left(B_k^T + A_k^T K_{13}\right) - dc_{k-1}^{(\alpha)} H^T - F_k^T - bG_k^T + \left(c + dc_0^{(\alpha)}\right) B_k^T. \tag{3.61}$$

Therefore, the matrix form of the numerical scheme is.

$$\left[aI + bK_{12}^T - \left(c + dc_0^{(\alpha)}\right) K_{13}^T\right] A_k = d\sum_{j=1}^{k-1} \left(c_{k-j}^{(\alpha)} - c_{k-j-1}^{(\alpha)}\right) \left(B_k + K_{13}^T A_k\right) - dc_{k-1}^{(\alpha)} H - F_k - bG_k + \left(c + dc_0^{(\alpha)}\right) B_k. \tag{3.62}$$

Solving the system of algebraic equation (3.62), we get A_k whose elements are unknown Legendre's coefficients a_{ij}. Putting the value of A_k, B_k, K_{13} in $\mathcal{U}^k(x) \approx \left(B_k^T + A_k^T K_{13}\right) \Psi(x)$ to get the approximate solution at each time level t_k. The advantage of using a meshfree operational matrix approach we get the solution at any point in the spatial domain.

The numerical algorithm for solving TFBSM by the proposed scheme (3.62) is given below.

Algorithm 3: To evaluate the numerical solution of TFBSM (3.10)-(3.12)

Input: The constants $a, b, c, \mathcal{H}(x), \mathcal{G}_1(t_k), \mathcal{G}_2(t_k), f(x), w(x), \alpha \in (0,1)$.

Output: The approximate solutions at each time level
$\mathcal{U}^k(x) \approx \left(B_k^T + A_k^T K_{13}\right) \Psi(x)$.

for Numeical solution of TFBSM by the semi-discrete scheme **do**

Step-1.1 Consider the uniform mesh in time domain $t_k = k\Delta t \ k = 0, 1, \ldots N$. Approximate the Caputo time-fractional derivative by L1-2 approximation, we transform the TFBSM in a function of space variable 'x' at each time level t_k.

Step-1.2 Generate the basis function $\psi_i(x)$; $i = 0, \ldots, M$ by using shifted Legendre polynomial as given in Section 3.3.1.

Step-1.3 By using boundary conditions $\mathcal{U}(x_L, t_k) = \mathcal{G}_1(t_k)$ and $\mathcal{U}(x_R, t_k) = \mathcal{G}_2(t_k)$, compute the operational vector G_k^T and B_k^T as defined in Remark 3.5.

Step-1.4 With the help of source term $f(x, t_k)$, compute the operational vector F_k^T and by using initial condition $\mathcal{U}(x, 0)$, compute H^T as given in Remark 3.6.

Step-1.5 Compute the operational matrix of integration K_1, K_1^2, K_2, K_3 of order $(M+1)$ as defined in Remark 3.7.

Step-1.6 Compute $K_{12} = K_1 - K_2$ and $K_{13} = K_1^2 - K_3$.

Step-1.7 Assuming $\mathcal{U}_{xx}^k(x) \approx A^T \psi(x)$ we get $\mathcal{U}_x^k(x) \approx \left(G_k^T + A_k^T K_{12}\right) \Psi(x)$ and $\mathcal{U}^k(x) \approx \left(B_k^T + A_k^T K_{13}\right) \Psi(x) \quad i = 1, \ldots, N-1$.

Step-1.8 Using Step-1.7 in Step (1.1), we get the matrix form of the numerical scheme at each time level k given in (3.62).

Step-1.9 Solving the system of equations (3.62) we get the value of unknown vector A_k at each time level k.

Step-1.10 Put the value of A_k, B_k, K_{13} in $\mathcal{U}^k(x) \approx \left(B_k^T + A_k^T K_{13}\right) \Psi(x)$ to get the approximate solution at each time level t_k.

end

Remark 3.8. The algorithm will remain same in case of second kind SCP basis function $\Phi(x)$. Only the basis $\Psi(x)$ has been replaced with $\Phi(x)$ with its respective weight function $w(x) = \sqrt{x - x^2}$.

3.5 Stability and convergence analysis of the numerical scheme

3.5.1 Stability analysis

The TFBSM is given as

$$ {}_0^C D_t^\alpha \mathcal{U}(x,t) = a\frac{\partial^2 \mathcal{U}(x,t)}{\partial x^2} + b\frac{\partial \mathcal{U}(x,t)}{\partial x} - c\mathcal{U}(x,t) + f(x,t), \tag{3.63} $$

with boundary and initial conditions

$$ \mathcal{U}(x_L,t) = \mathcal{G}_1(t),\ \mathcal{U}(x_R,t) = \mathcal{G}_2(t), \tag{3.64} $$

$$ \mathcal{U}(x,0) = \mathcal{H}(x). \tag{3.65} $$

For convenience and without loss of generality, we suppose $f = 0$ and $0 \leq a \leq 1$ & $0 \leq c \leq 1$ in (3.63) and discritizing the time direction by L1-2 approximation, we get

$$ {}_0\mathbb{D}_t^\alpha \mathcal{U}(x,t_k) = \frac{\partial^2 \mathcal{U}(x,t_k)}{\partial x^2} + b\frac{\partial \mathcal{U}(x,t_k)}{\partial x} - \mathcal{U}(x,t_k). \tag{3.66} $$

From (3.14), the L1-2 approximation is given by

$$ \begin{aligned} {}_0\mathbb{D}_t^\alpha \mathcal{U}(x,t_k) &= \frac{\tau^{1-\alpha}}{\Gamma(2-\alpha)} \sum_{j=1}^{k} c_{k-j}^{(\alpha)} \delta_t \mathcal{U}^{j-\frac{1}{2}}(x), \\ &= d\sum_{j=0}^{k-1} c_k^{(\alpha)} (\mathcal{U}^{k-j}(x) - \mathcal{U}^{k-j-1}(x)), \end{aligned} \tag{3.67} $$

where, $d = \dfrac{\tau^{-\alpha}}{\Gamma(2-\alpha)}$. Therefore, another form of L1-2 approximation can be written as

$$ {}_0\mathbb{D}_t^{\alpha}\mathcal{U}(x,t_k) = d\left[c_0^{(\alpha)}\mathcal{U}^k(x) - (c_0^{(\alpha)} - c_1^{(\alpha)})\mathcal{U}^{k-1}(x) - \sum_{j=1}^{k-2}(c_j^{(\alpha)} - c_{j+1}^{(\alpha)})\mathcal{U}^{k-j-1}(x) - c_{k-1}^{(\alpha)}\mathcal{U}^0(x)\right]. \tag{3.68} $$

Using expression (3.67) in (3.66), we get,

$$ d\sum_{j=0}^{k-1} c_j^{(\alpha)}(\mathcal{U}^{k-j}(x) - \mathcal{U}^{k-j-1}(x)) = \frac{\partial^2\mathcal{U}^k(x)}{\partial x^2} + b\frac{\partial\mathcal{U}^k(x)}{\partial x} - \mathcal{U}^k(x). \tag{3.69} $$

The semi-discrete form of the TFBSM (3.63) is given by,

$$ dc_0^{(\alpha)}\mathcal{U}^k - a\frac{\partial^2\mathcal{U}^k}{\partial x^2} - b\frac{\partial\mathcal{U}^k}{\partial x} + c\mathcal{U}^k = d\left[(c_0^{(\alpha)} - c_1^{(\alpha)})\mathcal{U}^{k-1} + \sum_{j=1}^{k-2}(c_j^{(\alpha)} - c_{j+1}^{(\alpha)})\mathcal{U}^{k-j-1} + c_{k-1}^{(\alpha)}\mathcal{U}^0\right]. \tag{3.70} $$

For $k = 1$,

$$ dc_0^{(\alpha)}\mathcal{U}^1 - \frac{\partial^2\mathcal{U}^1}{\partial x^2} - b\frac{\partial\mathcal{U}^1}{\partial x} + \mathcal{U}^1 = dc_0^{(\alpha)}\mathcal{U}^0. \tag{3.71} $$

Now,we define some functional space equipped with standard norms and inner products as

$$ H^1(\Omega) = \left\{v \in L^2(\Omega), \frac{dv}{dx} \in L^2(\Omega)\right\}, \tag{3.72} $$

$$ H_0^1(\Omega) = \left\{v \in H^1(\Omega), v|_{\partial\Omega} = 0\right\}, \tag{3.73} $$

$$ H^m(\Omega) = \left\{v \in L^2(\Omega), \frac{d^k v}{dx^k} \in L^2(\Omega) \ \text{ for all +ve integer } k \le m\right\}, \tag{3.74} $$

where, $L^2(\Omega)$ is the space of measurable functions whose square is Lebesgue integrable in Ω. The inner product of $L^2(\Omega)$ and $H^1(\Omega)$ are defined as follows

$$\langle u, v\rangle_0 = \int_\Omega uv\ dx, \tag{3.75}$$

$$\langle u, v\rangle_1 = \langle u, v\rangle_0 + \left\langle \frac{du}{dx}, \frac{dv}{dx} \right\rangle_0, \tag{3.76}$$

and the corresponding norm is defined by

$$\|u\|_0 = \langle u, v\rangle_0^{1/2}, \quad \|u\|_1 = \langle u, v\rangle_1^{1/2}, \tag{3.77}$$

also, the norm $\|.\|_m$ of $H^m(\Omega)$ is defined by $\|v\|_m = \left(\sum_{k=0}^m \left\|\frac{d^k v}{dx^k}\right\|_0^2\right)^{1/2}$.
In this paper, we take the norm which is equivalent to the standard H_1 norm [42, 172]

$$\|v\|_1 = \left(\|v\|_0 + \alpha_0 \left\|\frac{dv}{dx}\right\|_0^2\right)^{1/2}, \tag{3.78}$$

where, $0 < \alpha_0 = \dfrac{a}{dc_0^{(\alpha)}} < 1$ for $\alpha \in (0, 1)$ and $d = \dfrac{\tau^{-\alpha}}{\Gamma(2-\alpha)}$.

Theorem 3.9. *The semi-discrete form (3.70) is unconditionally stable when* $0 < \alpha \leq \bar{\alpha}$ *i.e. for all* $\Delta t > 0$

$$\|\mathcal{U}^k\|_1 \leq \|\mathcal{U}^0\|_0, \quad k = 1, 2, \ldots, N. \tag{3.79}$$

Proof. We will prove this theorem by using the principle of mathematical induction. For k=1, Multiplying (3.71) by 'v'$\in H_0^1(\Omega)$ and integrating over the Ω, we get

$$dc_0^{(\alpha)}\langle \mathcal{U}^1, v\rangle + a\left\langle \frac{\partial \mathcal{U}^1}{\partial x}, \frac{\partial v}{\partial x}\right\rangle + b\left\langle \mathcal{U}^1, \frac{\partial v}{\partial x}\right\rangle + c\langle \mathcal{U}^1, v\rangle = dc_0^{(\alpha)}\langle \mathcal{U}^0, v\rangle, \tag{3.80}$$

putting $v = \mathcal{U}^1$ in (3.80),

$$dc_0^{(\alpha)}\langle \mathcal{U}^1, \mathcal{U}^1\rangle + a\left\langle \frac{\partial \mathcal{U}^1}{\partial x}, \frac{\partial \mathcal{U}^1}{\partial x}\right\rangle + b\left\langle \mathcal{U}^1, \frac{\partial \mathcal{U}^1}{\partial x}\right\rangle + c\langle \mathcal{U}^1, \mathcal{U}^1\rangle = dc_0^{(\alpha)}\langle \mathcal{U}^0, \mathcal{U}^1\rangle. \tag{3.81}$$

Suppose $\left\langle \mathcal{U}^1, \frac{\partial \mathcal{U}^1}{\partial x}\right\rangle \geq 0$ for $k = 1, 2, \ldots, N$. Therefore

$$(c + dc_0^{(\alpha)})\|\mathcal{U}^1\|_0^2 + a\left\|\frac{\partial \mathcal{U}^1}{\partial x}\right\|_0^2 \leq dc_0^{(\alpha)}\|\mathcal{U}^0\|_0\|\mathcal{U}^1\|_0. \tag{3.82}$$

From (3.78), using the inequality $\|v\|_0 \leq \|v\|_1$, we get

$$\|\mathcal{U}^1\|_0^2 + \frac{a}{(c + dc_0^{(\alpha)})}\left\|\frac{\partial \mathcal{U}^1}{\partial x}\right\|_0^2 \leq \frac{dc_0^{(\alpha)}}{(c + dc_0^{(\alpha)})}\|\mathcal{U}^0\|_0\|\mathcal{U}^1\|_1 \leq \|\mathcal{U}^0\|_0\|\mathcal{U}^1\|_1,$$

$$\|\mathcal{U}^1\|_0^2 + \frac{a}{(c + dc_0^{(\alpha)})}\left\|\frac{\partial \mathcal{U}^1}{\partial x}\right\|_0^2 \leq \|\mathcal{U}^1\|_0^2 + \alpha_0\left\|\frac{\partial \mathcal{U}^1}{\partial x}\right\|_0^2 \leq \|\mathcal{U}^0\|_0\|\mathcal{U}^1\|_1,$$

$$\|\mathcal{U}^1\|_1^2 \leq \|\mathcal{U}^0\|_0\|\mathcal{U}^1\|_1,$$

$$\|\mathcal{U}^1\|_1 \leq \|\mathcal{U}^0\|_0. \tag{3.83}$$

Hence, the inequality (3.79) holds for $k = 1$.

Now, suppose the relation (3.79) is true for $k = 2, 3, \ldots, N-1$. i.e.

$$\|\mathcal{U}^k\|_1 \leq \|\mathcal{U}^0\|_0, \quad k = 2, 3, \ldots, N-1. \tag{3.84}$$

Then, multiplying (3.70) by 'v' and integrating over the domain Ω, we get,

$$dc_0^{(\alpha)}\langle \mathcal{U}^k, v\rangle + a\left\langle \frac{\partial \mathcal{U}^k}{\partial x}, \frac{\partial v}{\partial x}\right\rangle + b\left\langle \mathcal{U}^k, \frac{\partial v}{\partial x}\right\rangle + c\langle \mathcal{U}^k, v\rangle = d(c_0^{(\alpha)} - c_1^{(\alpha)})\langle \mathcal{U}^{k-1}, v\rangle + d\sum_{j=1}^{k-2}(c_j^{(\alpha)} - c_{j+1}^{(\alpha)})\langle \mathcal{U}^{k-j-1}, v\rangle + dc_{k-1}^{(\alpha)}\langle \mathcal{U}^0, v\rangle. \tag{3.85}$$

Putting $v = \mathcal{U}^k$ in (3.85)

$$dc_0^{(\alpha)}\langle \mathcal{U}^k, \mathcal{U}^k\rangle + a\left\langle \frac{\partial \mathcal{U}^k}{\partial x}, \frac{\partial \mathcal{U}^k}{\partial x}\right\rangle + b\left\langle \mathcal{U}^k, \frac{\partial \mathcal{U}^k}{\partial x}\right\rangle + c\langle \mathcal{U}^k, \mathcal{U}^k\rangle = d(c_0^{(\alpha)} - c_1^{(\alpha)})\langle \mathcal{U}^{k-1}, \mathcal{U}^k\rangle + d\sum_{j=1}^{k-2}(c_j^{(\alpha)} - c_{j+1}^{(\alpha)})\langle \mathcal{U}^{k-j-1}, \mathcal{U}^k\rangle + dc_{k-1}^{(\alpha)}\langle \mathcal{U}^0, \mathcal{U}^k\rangle, \tag{3.86}$$

$$(c + dc_0^{(\alpha)})\|\mathcal{U}^k\|_0^2 + a\left\|\frac{\partial \mathcal{U}^k}{\partial x}\right\|_0^2 \le d(c_0^{(\alpha)} - c_1^{(\alpha)})\|\mathcal{U}^{k-1}\|_0\|\mathcal{U}^k\|_0 + d\sum_{j=1}^{k-2}(c_j^{(\alpha)} - c_{j+1}^{(\alpha)})\|\mathcal{U}^{k-j-1}\|_0\|\mathcal{U}^k\|_0 + dc_{k-1}^{(\alpha)}\|\mathcal{U}^0\|_0\|\mathcal{U}^k\|_0.$$

Now, using the inequality $\|v^k\|_0 \le \|v^k\|_1$ in above equation, we get,

$$(c + dc_0^{(\alpha)})\|\mathcal{U}^k\|_0^2 + a\left\|\frac{\partial \mathcal{U}^k}{\partial x}\right\|_0^2 \le d(c_0^{(\alpha)} - c_1^{(\alpha)})\|\mathcal{U}^{k-1}\|_1\|\mathcal{U}^k\|_1 + d\sum_{j=1}^{k-2}(c_j^{(\alpha)} - c_{j+1}^{(\alpha)})\|\mathcal{U}^{k-j-1}\|_1\|\mathcal{U}^k\|_1 + dc_{k-1}^{(\alpha)}\|\mathcal{U}^0\|_1\|\mathcal{U}^k\|_1.$$

Now, by the assumption (3.84)

$$(c+dc_0^{(\alpha)})\|\mathcal{U}^k\|_0^2 + a\left\|\frac{\partial \mathcal{U}^k}{\partial x}\right\|_0^2 \leq d(c_0^{(\alpha)} - c_1^{(\alpha)})\|\mathcal{U}^0\|_0\|\mathcal{U}^k\|_1 + d\sum_{j=1}^{k-2}(c_j^{(\alpha)} - c_{j+1}^{(\alpha)})\|\mathcal{U}^0\|_0\|\mathcal{U}^k\|_1 + dc_{k-1}^{(\alpha)}\|\mathcal{U}^0\|_0\|\mathcal{U}^k\|_1.$$

The above equation can be re-written as

$$\|\mathcal{U}^k\|_0^2 + \frac{a}{(c+dc_0^{(\alpha)})}\left\|\frac{\partial \mathcal{U}^k}{\partial x}\right\|_0^2 \leq \frac{d}{(c+dc_0^{(\alpha)})}\left[(c_0^{(\alpha)} - c_1^{(\alpha)}) + \sum_{j=1}^{k-2}(c_j^{(\alpha)} - c_{j+1}^{(\alpha)}) + c_{k-1}^{(\alpha)}\right]\|\mathcal{U}^0\|_0\|\mathcal{U}^k\|_1,$$

$$\|\mathcal{U}^k\|_1^2 \leq \frac{dc_0^{(\alpha)}}{(c+dc_0^{(\alpha)})}\|\mathcal{U}^0\|_0\|\mathcal{U}^k\|_1 \leq \|\mathcal{U}^0\|_0\|\mathcal{U}^k\|_1,$$

$$\|\mathcal{U}^k\|_1^2 \leq \|\mathcal{U}^0\|_0\|\mathcal{U}^k\|_1,$$

$$\|\mathcal{U}^k\|_1 \leq \|\mathcal{U}^0\|_0. \tag{3.87}$$

Which proves the theorem. □

Remark 3.10. We have established unconditionally stability only for $0 < \alpha \leq \bar{\alpha}$ because $c_1^{(\alpha)} - c_2^{(\alpha)} \geq 0$ if $0 < \alpha \leq \bar{\alpha}$ (see Lemma (3.2)).

Remark 3.11. When $\alpha \in (\bar{\alpha}, 1)$ then $c_1^{(\alpha)} - c_2^{(\alpha)} < 0$, therefore (3.85) does not imply (3.86). A different approach is needed in this case, which is under investigation. Therefore we have showed the numerical stability for $\alpha \in (\bar{\alpha}, 1)$ and found that the numerical scheme is completely stable for all $\alpha \in (0, 1)$.

Now we find the error estimate of the semi-discretized scheme.

3.5.2 Convergence analysis

Theorem 3.12. *Let* $\mathcal{U}(t_k)$ *be the exact solution of the TFBSM (3.63) and* $\mathcal{U}^k$ *be the time-discrete solution of equation (3.86) with initial condition* $\mathcal{U}^0 = \mathcal{U}(x,0)$*, then the following error estimate holds for* $0 < \alpha \leq \bar{\alpha}$

1. $\|\mathcal{U}(t_1) - \mathcal{U}^1\|_1 \leq \dfrac{1}{c_0^{(\alpha)}} E_\alpha M(\mathcal{U}) T^\alpha \tau^{2-\alpha}$,
2. $\|\mathcal{U}(t_k) - \mathcal{U}^k\|_1 \leq \dfrac{k^{-\alpha}}{c_{k-2}^{(\alpha)}} \tilde{E}_\alpha \tilde{M}(\mathcal{U}) T^\alpha \tau^{3-\alpha}, \ k \geq 2.$

where $C_\alpha = \dfrac{\alpha}{2\Gamma(3-\alpha)}$, $\tilde{C}_\alpha = \left[\dfrac{1}{12\Gamma(1-\alpha)} + \dfrac{\alpha(5-\alpha)}{6\Gamma(4-\alpha)}\right]$, $E_\alpha = \Gamma(2-\alpha)C_\alpha$, $\tilde{E}_\alpha = \Gamma(2-\alpha)\tilde{C}_\alpha$, $M(\mathcal{U}) = \max_{t_0 \leq t \leq t_1} |\mathcal{U}''(t)|$, $\tilde{M}(\mathcal{U}) = \max_{t_0 \leq t \leq t_k} |\mathcal{U}'''(t)|$.

Proof. Let $e^k = \mathcal{U}(x,t_k) - \mathcal{U}^k(x)$ denotes the error at time level k then from (3.23)

$$r_\tau^k = {}_0^C D_t^\alpha \mathcal{U}(t)|_{t=t_k} - {}_0\mathbb{D}_t^\alpha \mathcal{U}(t)|_{t=t_k}. \tag{3.88}$$

Since, the TFBSM at time level t_k is given by

$${}_0^C D_t^\alpha \mathcal{U}(x,t_k) - a\frac{\partial^2 \mathcal{U}(x,t_k)}{\partial x^2} - b\frac{\partial \mathcal{U}(x,t_k)}{\partial x} + c\mathcal{U}(x,t_k) = 0. \tag{3.89}$$

Using L1-2 approximation, we get

$${}_0\mathbb{D}_t^\alpha \mathcal{U}(x,t_k) - a\frac{\partial^2 \mathcal{U}(x,t_k)}{\partial x^2} - b\frac{\partial \mathcal{U}(x,t_k)}{\partial x} + c\mathcal{U}(x,t_k) = -r_\tau^k, \tag{3.90}$$

$${}_0\mathbb{D}_t^\alpha \mathcal{U}^k(x) - a\frac{\partial^2 \mathcal{U}^k(x)}{\partial x^2} - b\frac{\partial \mathcal{U}^k(x)}{\partial x} + c\mathcal{U}^k(x) = 0. \tag{3.91}$$

Subtracting (3.90) and (3.91), we get

$$ {}_0\mathbb{D}_t^{\alpha}(\mathcal{U}(x,t_k)-\mathcal{U}^k(x))-a\frac{\partial^2}{\partial x^2}(\mathcal{U}(x,t_k)-\mathcal{U}^k(x))-b\frac{\partial}{\partial x}(\mathcal{U}(x,t_k)-\mathcal{U}^k(x)) $$
$$ +c(\mathcal{U}(x,t_k)-\mathcal{U}^k(x))=-r_\tau^k, $$

$$ {}_0\mathbb{D}_t^{\alpha}e^k-a\frac{\partial^2 e^k}{\partial x^2}-b\frac{\partial e^k}{\partial x}+ce^k=-r_\tau^k. \tag{3.92} $$

Using (3.67) and multiplying by 'v'$\in H_0^1(\Omega)$ and integrating over the domain Ω, we get

$$ dc_0^{(\alpha)}\langle e^k,v\rangle+a\left\langle\frac{\partial e^k}{\partial x},\frac{\partial v}{\partial x}\right\rangle+b\left\langle e^k,\frac{\partial v}{\partial x}\right\rangle+c\langle e^k,v\rangle= $$
$$ d(c_0^{(\alpha)}-c_1^{(\alpha)})\langle e^{k-1},v\rangle+d\sum_{j=1}^{k-2}(c_j^{(\alpha)}-c_{j+1}^{(\alpha)})\langle e^{k-j-1},v\rangle+dc_{k-1}^{(\alpha)}\langle e^0,v\rangle-\langle r_\tau^k,v\rangle. \tag{3.93} $$

Let $v=e^k$, and since $e^0=\mathcal{U}(x,0)-\mathcal{U}^0(x)=0$, therefore

$$ dc_0^{(\alpha)}\langle e^k,e^k\rangle+a\left\langle\frac{\partial e^k}{\partial x},\frac{\partial e^k}{\partial x}\right\rangle+b\left\langle e^k,\frac{\partial e^k}{\partial x}\right\rangle+c\langle e^k,e^k\rangle= $$
$$ d(c_0^{(\alpha)}-c_1^{(\alpha)})\langle e^{k-1},e^k\rangle+d\sum_{j=1}^{k-2}(c_j^{(\alpha)}-c_{j+1}^{(\alpha)})\langle e^{k-j-1},e^k\rangle-\langle r_\tau^k,e^k\rangle. \tag{3.94} $$

Following the same process as in Theorem 3.9

$$ (c+dc_0^{(\alpha)})\|e^k\|_0^2+a\left\|\frac{\partial e^k}{\partial x}\right\|_0^2\le d(c_0^{(\alpha)}-c_1^{(\alpha)})\|e^{k-1}\|_0\|e^k\|_0+d\sum_{j=1}^{k-2}(c_j^{(\alpha)}-c_{j+1}^{(\alpha)})\|e^{k-j-1}\|_0\|e^k\|_0 $$
$$ +dc_{k-1}^{(\alpha)}\|e^0\|_0\|e^k\|_0-\|r_\tau^k\|_0\|e^k\|_0. \tag{3.95} $$

Now, using the inequality $\|v^k\|_0 \leq \|v^k\|_1$ in (3.95), we get

$$(c+dc_0^{(\alpha)})\|e^k\|_0^2 + a\left\|\frac{\partial e^k}{\partial x}\right\|_0^2 \leq d(c_0^{(\alpha)}-c_1^{(\alpha)})\|e^{k-1}\|_1\|e^k\|_1 + d\sum_{j=1}^{k-2}(c_j^{(\alpha)}-c_{j+1}^{(\alpha)})\|e^{k-j-1}\|_1\|e^k\|_1 + dc_{k-1}^{(\alpha)}\|e^0\|_1\|e^k\|_1 - \|r_\tau^k\|_0\|e^k\|_1, \tag{3.96}$$

$$\|e^k\|_0^2 + \frac{a}{(c+dc_0^{(\alpha)})}\left\|\frac{\partial e^1}{\partial x}\right\|_0^2 \leq \frac{1}{(c+dc_0^{(\alpha)})}\Bigg[d(c_0^{(\alpha)}-c_1^{(\alpha)})\|e^{k-1}\|_1\|e^k\|_1 + d\sum_{j=1}^{k-2}(c_j^{(\alpha)}-c_{j+1}^{(\alpha)})\|e^{k-j-1}\|_1\|e^k\|_1 + dc_{k-1}^{(\alpha)}\|e^0\|_1\|e^k\|_1 - \|r_\tau^k\|_0\|e^k\|_1\Bigg], \tag{3.97}$$

$$\|e^k\|_1^2 \leq \frac{1}{dc_0^{(\alpha)}}\left[d(c_0^{(\alpha)}-c_1^{(\alpha)})\|e^{k-1}\|_1 + d\sum_{j=1}^{k-2}(c_j^{(\alpha)}-c_{j+1}^{(\alpha)})\|e^{k-j-1}\|_1 + dc_{k-1}^{(\alpha)}\|e^0\|_1 - \|r_\tau^k\|_0\right]\|e^k\|_1, \tag{3.98}$$

$$\|e^k\|_1 \leq \frac{1}{c_0^{(\alpha)}}\left[(c_0^{(\alpha)}-c_1^{(\alpha)})\|e^{k-1}\|_1 + \sum_{j=1}^{k-2}(c_j^{(\alpha)}-c_{j+1}^{(\alpha)})\|e^{k-j-1}\|_1 + c_{k-1}^{(\alpha)}\|e^0\|_1\right] - \frac{1}{dc_0^{(\alpha)}}\|r_\tau^k\|_0. \tag{3.99}$$

(1) Putting $k=1$, the (3.99) can be written as

$$\|e^1\|_1 \leq \frac{1}{c_0^{(\alpha)}}c_0^{(\alpha)}\|e^0\|_1 - \frac{1}{dc_0^{(\alpha)}}\|r_\tau^1\|_0.$$

Since $\|e^0\|_1 = 0$, therefore

$$\|e^1\|_1 \leq \frac{1}{dc_0^{(\alpha)}}\|r_\tau^1\|_0 \leq \frac{\Gamma(2-\alpha)\tau^\alpha}{c_0^{(\alpha)}}C_\alpha M(\mathcal{U})\tau^{2-\alpha},$$

$$\|e^1\|_1 \leq \frac{1}{c_0^{(\alpha)}} E_\alpha M(\mathcal{U})\tau^2 = \frac{(k\tau)^\alpha}{c_0^{(\alpha)}} E_\alpha M(\mathcal{U})\tau^{2-\alpha}, \tag{3.100}$$

For $k = 1$, $k\tau = T$,

$$\|\mathcal{U}(t_1) - \mathcal{U}^1\|_1 \leq \frac{1}{c_0^{(\alpha)}} E_\alpha M(\mathcal{U}) T^\alpha \tau^{2-\alpha}. \tag{3.101}$$

This proves the first part of the theorem.

(2) Now, for $2 \leq j \leq k$, we will first prove the following inequality by mathematical induction

$$\|e^j\|_1 \leq \frac{1}{c_{j-2}^{(\alpha)}} \tilde{E}_\alpha \tilde{M}(\mathcal{U})\tau^3. \tag{3.102}$$

Putting $j = 2$ in (3.99), we obtain

$$\|e^2\|_1 \leq \frac{1}{c_0^{(\alpha)}} \left[(c_0^{(\alpha)} - c_1^{(\alpha)})\|e^1\|_1 + c_1^{(\alpha)}\|e^0\|_1\right] - \frac{1}{dc_0^{(\alpha)}}\|r_\tau^2\|_0. \tag{3.103}$$

By using (3.100) and Theorem (3.3), we get

$$\|e^2\|_1 \leq \frac{1}{c_0^{(\alpha)}} \left[(c_0^{(\alpha)} - c_1^{(\alpha)})\frac{1}{c_0^{(\alpha)}} E_\alpha M(\mathcal{U})\tau^2\right] - \frac{1}{dc_0^{(\alpha)}} \left[C_\alpha M(\mathcal{U})\tau^{2-\alpha} + \tilde{C}_\alpha \tilde{M}(\mathcal{U})\tau^{3-\alpha}\right]. \tag{3.104}$$

Since $c_1^{(\alpha)} > 0$ for $\alpha < 0.68029$ (Lemma 3.2), therefore adding the term $\frac{c_1^{(\alpha)}}{c_0^{(\alpha)}} E_\alpha M(\mathcal{U})\tau^2 > 0$ on the R.H.S. does not affect the inequality (3.104)

$$\|e^2\|_1 \leq \frac{1}{c_0^{(\alpha)}} \left[(c_0^{(\alpha)} - c_1^{(\alpha)})\frac{1}{c_0^{(\alpha)}} E_\alpha M(\mathcal{U})\tau^2 + \frac{c_1^{(\alpha)}}{c_0^{(\alpha)}} E_\alpha M(\mathcal{U})\tau^2\right] - \frac{1}{c_0^{(\alpha)}} E_\alpha M(\mathcal{U})\tau^2 - \frac{1}{c_0^{(\alpha)}} \tilde{E}_\alpha \tilde{M}(\mathcal{U})\tau^3. \tag{3.105}$$

Simplifying (3.105), we get

$$\|e^2\|_1 \leq \frac{1}{c_0^{(\alpha)}} \tilde{E}_\alpha \tilde{M}(\mathcal{U})\tau^3. \tag{3.106}$$

Thus, the inequality (3.102) is true for $j = 2$. Now, suppose the inequality (3.102) is true for $j = 3, 4, \ldots, k-1$. Now, to prove that the inequality (3.102) is true for $j = k$, we have from (3.99)

$$\|e^k\|_1 \leq \frac{1}{c_0^{(\alpha)}} \left[(c_0^{(\alpha)} - c_1^{(\alpha)})\|e^{k-1}\|_1 + \sum_{j=1}^{k-2} (c_j^{(\alpha)} - c_{j+1}^{(\alpha)})\|e^{k-j-1}\|_1 + c_{k-1}^{(\alpha)}\|e^0\|_1 \right] - \frac{1}{dc_0^{(\alpha)}}\|r_\tau^k\|_0. \tag{3.107}$$

Since, $\|e^0\|_1 = 0$, therefore,

$$\|e^k\|_1 \leq \frac{1}{c_0^{(\alpha)}} \left[(c_0^{(\alpha)} - c_1^{(\alpha)})\|e^{k-1}\|_1 + \sum_{j=1}^{k-3} (c_j^{(\alpha)} - c_{j+1}^{(\alpha)})\|e^{k-j-1}\|_1 + (c_{k-2}^{(\alpha)} - c_{k-1}^{(\alpha)})\|e^1\|_1 \right] - \frac{1}{dc_0^{(\alpha)}}\|r_\tau^k\|_0. \tag{3.108}$$

Using (3.100) and (3.102) in (3.108),

$$\|e^k\|_1 \leq \frac{1}{c_0^{(\alpha)}} \left[(c_0^{(\alpha)} - c_1^{(\alpha)}) \frac{1}{c_{k-3}^{(\alpha)}} \tilde{E}_\alpha \tilde{M}(\mathcal{U})\tau^3 + \sum_{j=1}^{k-3} (c_j^{(\alpha)} - c_{j+1}^{(\alpha)}) \frac{1}{c_{k-j-3}^{(\alpha)}} \tilde{E}_\alpha \tilde{M}(\mathcal{U})\tau^3 \right] + (c_{k-2}^{(\alpha)} - c_{k-1}^{(\alpha)}) \frac{1}{c_0^{(\alpha)}} E_\alpha M(\mathcal{U})\tau^2 - \frac{1}{dc_0^{(\alpha)}} \left[C_\alpha M(\mathcal{U})\tau^{2-\alpha} + \tilde{C}_\alpha \tilde{M}(\mathcal{U})\tau^{3-\alpha} \right]. \tag{3.109}$$

From Lemma (3.2) for $0 < \alpha < \bar{\alpha}$, $\frac{1}{c_0^\alpha} \leq \frac{1}{c_1^\alpha} \leq \ldots \frac{1}{c_{k-2}^\alpha} \leq \frac{1}{c_{k-1}^\alpha}$ and also adding two term $\frac{c_{k-2}^{(\alpha)}}{c_{k-2}^{(\alpha)}} \tilde{E}_\alpha M(\mathcal{U})\tau^3 > 0$ and $\frac{c_{k-1}^{(\alpha)}}{c_{k-2}^{(\alpha)}} E_\alpha M(\mathcal{U})\tau^2 > 0$ on the R.H.S. of (3.109), we get,

$$\begin{aligned}\|e^k\|_1 \leq & \frac{1}{c_0^{(\alpha)}}\Bigg[(c_0^{(\alpha)} - c_1^{(\alpha)})\frac{1}{c_{k-2}^{(\alpha)}}\tilde{E}_\alpha \tilde{M}(\mathcal{U})\tau^3 + \sum_{j=1}^{k-3}(c_j^{(\alpha)} - c_{j+1}^{(\alpha)})\frac{1}{c_{k-2}^{(\alpha)}}\tilde{E}_\alpha \tilde{M}(\mathcal{U})\tau^3 + c_{k-2}^{(\alpha)}\frac{1}{c_{k-2}^{(\alpha)}}\tilde{E}_\alpha \tilde{M}(\mathcal{U})\tau^3 \\ & + (c_{k-2}^{(\alpha)} - c_{k-1}^{(\alpha)})\frac{1}{c_{k-2}^{(\alpha)}}E_\alpha M(\mathcal{U})\tau^2 + c_{k-1}^{(\alpha)}\frac{1}{c_{k-2}^{(\alpha)}}E_\alpha M(\mathcal{U})\tau^2\Bigg] - \frac{1}{c_0^{(\alpha)}}\left[E_\alpha M(\mathcal{U})\tau^2 + \tilde{E}_\alpha \tilde{M}(\mathcal{U})\tau^3\right].\end{aligned} \tag{3.110}$$

On simplifying, we get,

$$\|e^k\|_1 \leq \frac{1}{c_{k-2}^{(\alpha)}}\tilde{E}_\alpha \tilde{M}(\mathcal{U})\tau^3 - \frac{1}{c_0^{(\alpha)}}\tilde{E}_\alpha \tilde{M}(\mathcal{U})\tau^3, \tag{3.111}$$

$$\|e^k\|_1 \leq \frac{1}{c_{k-2}^{(\alpha)}}\tilde{E}_\alpha \tilde{M}(\mathcal{U})\tau^3, \tag{3.112}$$

which implies that, by the principle of mathematical induction, inequality (3.102) is true for all k. Now,

$$\|\mathcal{U}(t_k) - \mathcal{U}^k\|_1 \leq \frac{k^{-\alpha}}{c_{k-2}^{(\alpha)}}\tilde{E}_\alpha \tilde{M}(\mathcal{U})k^\alpha \tau^3, \tag{3.113}$$

$$\|\mathcal{U}(t_k) - \mathcal{U}^k\|_1 \leq \frac{k^{-\alpha}}{c_{k-2}^{(\alpha)}}\tilde{E}_\alpha \tilde{M}(\mathcal{U})(k\tau)^\alpha \tau^{3-\alpha}, \tag{3.114}$$

$$\|\mathcal{U}(t_k) - \mathcal{U}^k\|_1 \leq \frac{k^{-\alpha}}{c_{k-2}^{(\alpha)}}\tilde{E}_\alpha \tilde{M}(\mathcal{U})T^\alpha \tau^{3-\alpha}. \tag{3.115}$$

This proves the second part of the Theorem 3.12. □

Remark 3.13. We have proved the theoretical convergence of the semi-discrete scheme (3.67) only for $0 < \alpha < \bar{\alpha}$, which is of order $(3-\alpha)$. The reason for this is we can use Lemma 3.2 in (3.109) only when $0 < \alpha \leq \bar{\alpha}$. This is the limitation of L1-2 approximation of the Caputo derivative of order $\alpha \in (0,1)$ in proving the theoretical convergence and stability of the numerical scheme for all α.

Remark 3.14. For $\alpha \in (\bar{\alpha}, 1)$ a different approach is needed to prove the convergence and stability of the numerical scheme. But we have found that the computational order of convergence of the numerical scheme is $(3-\alpha)$ in time for all α.

3.6 Numerical results and discussion

In this section, we give some numerical examples of the TFBSM for the European options to validate the error efficiency of the proposed numerical algorithm. Let $\mathcal{M}$ be the number of grid point in space domain and N is the number of grid point in time domain for the purpose of error calculation. The L_2 and L_∞ error at time T of the numerical algorithm is defined as

$$\|\mathcal{U} - \mathcal{U}_n\|_2 = \left(\sum_{i=1}^{\mathcal{M}} h |\mathcal{U}(x_i, T) - \mathcal{U}_n(x_i, T)|^2 \right)^{\frac{1}{2}} \tag{3.116}$$

$$\|\mathcal{U} - \mathcal{U}_n\|_\infty = \max_{0 \leq i \leq \mathcal{M}} |\mathcal{U}(x_i, T) - \mathcal{U}_n(x_i, T)|, \tag{3.117}$$

where, $\mathcal{U}(x,T)$ and $\mathcal{U}_n(x,T)$ be the exact and numerical solution at time T of the TFBSM. The order of convergence in temporal direction is defined as

$$\text{Order of convergence in temporal direction} = \frac{\log(err(N_1)/err(N_2))}{\log(N_1/N_2)}, \tag{3.118}$$

where, err(N_i) denotes the L_2 or L_∞ error at final time T corresponding to the grid points N_i.

3.6.1 Numerical stability

The stability of the numerical algorithms are verified numerically by adding some noisy data in the initial condition [166, 167]. Let $\mathcal{U}^\delta(x,0)$ denotes the initial condition with the noise δ i.e.

$$\mathcal{U}^\delta(x_i,0) = \mathcal{U}(x_i,0) + \delta\omega, \tag{3.119}$$

where, ω is the uniform random variable whose values lies in $[-1,1]$, such that

$$\max_{1\le i\le \mathcal{M}} (\mathcal{U}(x_i,0) - \mathcal{U}^\delta(x_i,0)) \le \delta. \tag{3.120}$$

Here, we will choose two different noise δ^i as $\delta^1 = m\%$ of $\mu^{\mathcal{M}}$ and $\delta^2 = \sigma^{\mathcal{M}}$, where $\mu^{\mathcal{M}}$ is the mean value of the initial values at each spatial grid points which is defined as

$$\mu^{\mathcal{M}} = \frac{1}{\mathcal{M}+1}\sum_{i=0}^{\mathcal{M}} \mathcal{U}(x_i,0), \tag{3.121}$$

and $\sigma^{\mathcal{M}}$ is the root mean square error and defined as

$$\sigma^{\mathcal{M}} = \left(\sum_{i=1}^{\mathcal{M}} h|\mathcal{U}(x_i,T) - \mathcal{U}_n(x_i,T)|^2\right)^{\frac{1}{2}}. \tag{3.122}$$

Remark 3.15. We have taken $m = 0.1$ and $\mathcal{M} = 100$ in the first two examples.

Remark 3.16. We have carried out the numerical experiments on a Laptop having processor Intel(R) Core (TM) i5-2430M CPU with speed 2.40 GHz and 8GB RAM

on a 64-bit operating system running on MATLAB 2015a (The MathWorks, Inc., Natick, Massachusetts) programming software.

3.6.2 Numerical examples for the TFBSM governing European options

Example 3.6.1. Consider the TFBSM (3.10) with initial condition $\mathcal{U}(x,0) = x^2(1-x)$, $(x,t) \in (0,1)\times(0,1)$, homogeneous boundary conditions $\mathcal{U}(0,t) = 0$, $\mathcal{U}(1,t) = 0$ and source function

$$f(x,t) = \left(\frac{2t^{2-\alpha}}{\Gamma(3-\alpha)} + \frac{2t^{1-\alpha}}{\Gamma(2-\alpha)}\right) x^2(1-x) - (t+1)^2\left[a(2-6x) + b(2x-3x^2) - cx^2(1-x)\right]. \tag{3.123}$$

The exact solution of Ex. 3.6.1 is,

$$\mathcal{U}(x,t) = (t+1)^2x^2(1-x). \tag{3.124}$$

Here, $\alpha = 0.7$, $\tau = 1/160$, $h = 0.05$, $M = 4$ SLP/SCP basis function, $T = 1$ and the parameter values are $r = 0.05$, $\sigma = 0.25$, $a = \frac{1}{2}\sigma^2$, $b = r - a$, $c = r$. The followings outcomes of Ex. 3.6.1 are:

- From fig. 3.1, it is observed that at each time level, approximate solutions are in good agreement with the exact solutions in the case of homogeneous conditions.
- Fig. 3.2 shows that the absolute error decreasing with increase in time level. The effect of fractional order α to the solution profile is reflected in fig. 3.3. It can be observed that the absolute error is decreasing with decrease in α.

τ	$\alpha = 0.1$			$\alpha = 0.5$			$\alpha = 0.9$		
	L_2 error	CO	CPU	L_2 error	CO	CPU	L_2 error	CO	CPU
1/10	1.816e-06	-	1.21	5.480e-05	-	1.21	5.893e-04	-	1.22
1/20	2.338e-07	2.958	1.82	9.340e-06	2.553	1.80	1.347e-04	2.129	1.88
1/40	3.054e-08	2.936	3.09	1.619e-06	2.528	3.07	3.114e-05	2.113	3.16
1/80	4.020e-09	2.926	6.11	2.832e-07	2.516	6.14	7.232e-06	2.106	6.19
1/160	5.312e-10	2.920	12.58	4.975e-08	2.509	12.52	1.683e-06	2.103	12.52

TABLE 3.1: L_2 error, order of convergence (CO) and CPU time (in seconds) for Ex. 3.6.1 using SLP basis at $T = 1$.

- **Numerical stability:** The stability of the proposed algorithm can be verified numerically in fig. 3.4. It shows the behavior of absolute errors in the absence of noise and also with addition of two different noise in the initial condition, $\delta^1 = 0.1\%\mu^{100}$ and $\delta^2 = 10\sigma^{100}$. It is observed that the variation in the absolute error with the presence of noise is almost negligible as compared to without noise. This verifies the stability of our numerical algorithm.

- From Tables 3.1-3.4, we conclude that L_2 and L_∞-error are almost the same with both the basis function but the CPU time taken by the SLP basis is less than SCP basis. The temporal order of convergence with respect to L_2-norm and L_∞-norm is of order $(3 - \alpha)$, which validates the theoretical results. .

- A comparative study of L_2 and L_∞ errors, obtained by the proposed algorithm and the scheme given in [1] and [2] is given in Table 3.5. It is observed from that the error efficiency of the proposed algorithm is better than earlier scheme.

- Table 3.6 indicates the pointwise absolute error (PAE) in spatial direction with respect to both the basis. The spatial accuracy also reaches from 10^{-6} to 10^{-10} for different values of α only using four number of basis functions. Also, the accuracy is almost uniform at each spatial grid point throughout the domain [0,1], for each α.

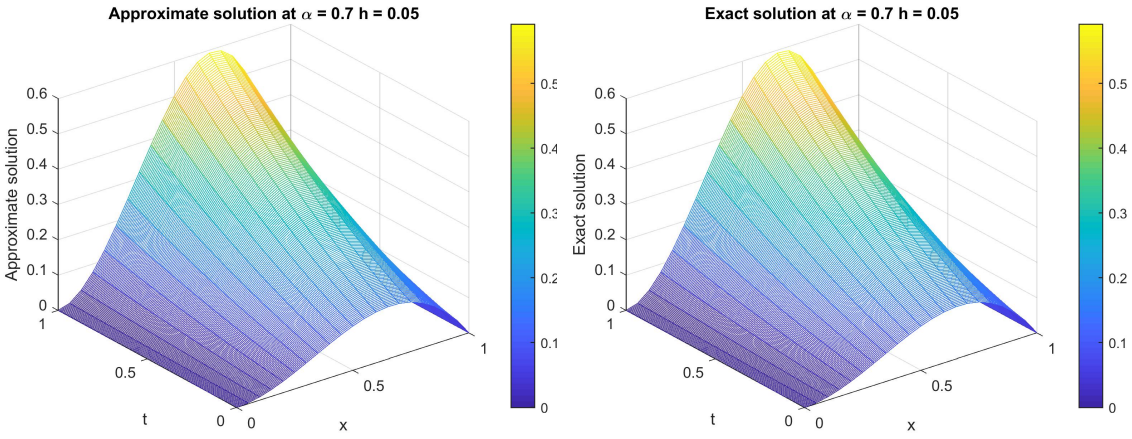

FIGURE 3.1: Surface plot of approximate solution (left) and exact solution (right) of Ex. 3.6.1 for $\alpha = 0.7$, $\tau = 1/160$ using $M = 4$ SLP basis

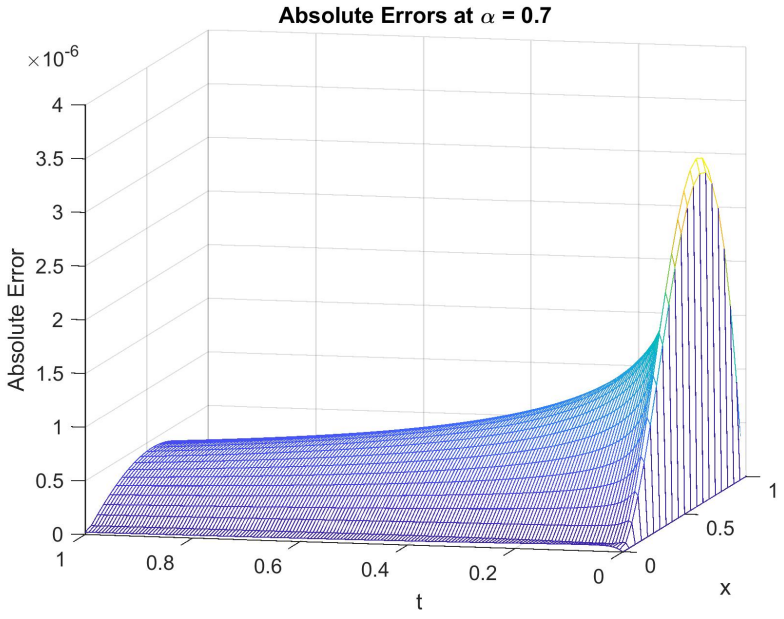

FIGURE 3.2: Absolute errors of Ex. 3.6.1 for $\alpha = 0.7$, $\tau = 1/160$ using $M = 4$ SLP basis.

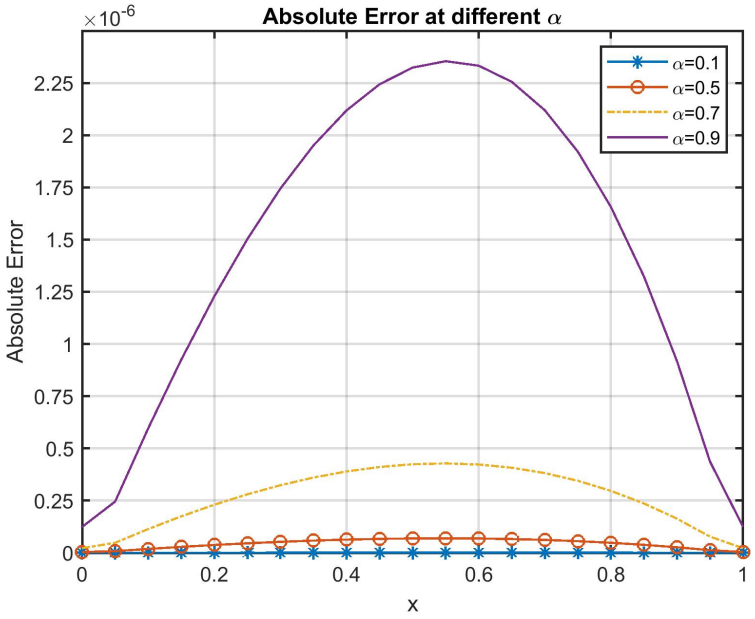

FIGURE 3.3: Absolute errors of Ex. 3.6.1 for different values of α at time $T = 1$ using $M = 4$ SLP basis.

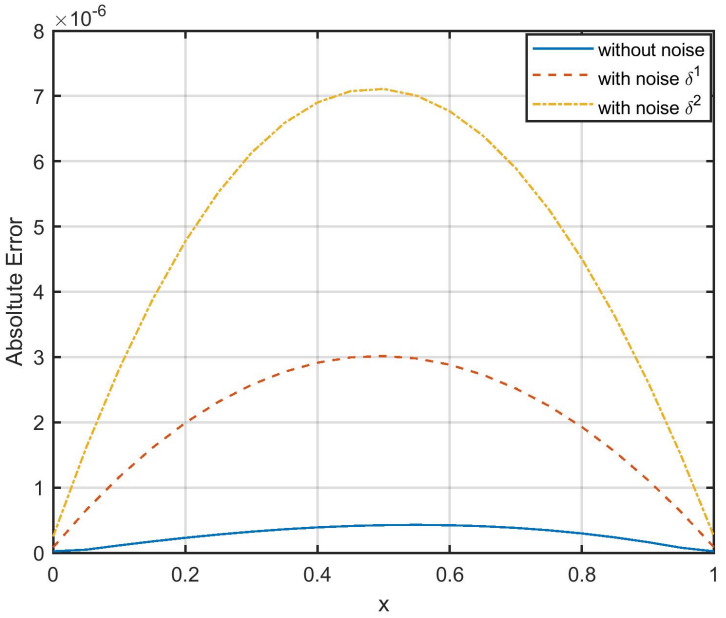

FIGURE 3.4: Absolute errors of Ex. 3.6.1 for $\alpha = 0.7$ with different noise using $M = 4$ SLP basis.

τ	$\alpha = 0.1$			$\alpha = 0.5$			$\alpha = 0.9$		
	L_∞ error	CO	CPU	L_∞ error	CO	CPU	L_∞ error	CO	CPU
1/10	2.663e-06	-	1.21	7.849e-05	-	1.21	8.494e-04	-	1.22
1/20	3.386e-07	2.959	1.82	1.337e-05	2.554	1.80	1.940e-04	2.131	1.88
1/40	4.418e-08	2.938	3.09	2.317e-06	2.529	3.07	4.481e-05	2.114	3.16
1/80	5.809e-09	2.927	6.11	4.050e-07	2.516	6.14	1.040e-06	2.107	6.19
1/160	7.668e-10	2.921	12.58	7.115e-08	2.509	12.52	2.421e-06	2.103	12.52

TABLE 3.2: L_∞ error, order of convergence (CO) and CPU time (in seconds) for Ex. 3.6.1 using SLP basis at $T = 1$.

τ	$\alpha = 0.1$			$\alpha = 0.5$			$\alpha = 0.9$		
	L_2 error	CO	CPU	L_2 error	CO	CPU	L_2 error	CO	CPU
1/10	1.806e-06	-	5.04	5.440e-05	-	5.00	5.852e-04	-	5.05
1/20	2.324e-07	2.957	8.02	9.271e-06	2.553	8.06	1.337e-04	2.129	8.00
1/40	3.037e-08	2.936	14.26	1.607e-06	2.528	14.20	3.091e-05	2.113	14.22
1/80	3.996e-09	2.925	28.05	2.810e-07	2.516	28.20	7.180e-06	2.106	28.38
1/160	5.280e-10	2.920	56.88	4.937e-08	2.508	56.67	1.671e-06	2.103	56.92

TABLE 3.3: L_2 error, order of convergence (CO) and CPU time (in seconds) for Ex. 3.6.1 using SCP basis at $T = 1$.

τ	$\alpha = 0.1$			$\alpha = 0.5$			$\alpha = 0.9$		
	L_∞ error	CO	CPU	L_∞ error	CO	CPU	L_∞ error	CO	CPU
1/10	2.581e-06	-	5.04	7.666e-05	-	5.00	8.284e-04	-	5.05
1/20	3.318e-07	2.957	8.02	1.305e-06	2.554	8.06	1.891e-04	2.171	8.00
1/40	4.329e-08	2.936	14.26	2.262e-06	2.528	14.20	4.369e-05	2.130	14.22
1/80	5.691e-09	2.925	28.05	3.954e-07	2.516	28.20	1.014e-06	2.114	28.38
1/160	7.511e-10	2.920	56.88	6.945e-08	2.509	56.67	2.360e-06	2.106	56.92

TABLE 3.4: L_∞ error, order of convergence (CO) and CPU time (in seconds) for Ex. 3.6.1 using SCP basis at $T = 1$

τ	L_2 Error		L_∞ Error		
	In [1]	Our Method	In [1]	In [2]	Our Method
1/10	0.0025	1.905e-04	0.0037	0.0035	2.732e-04
1/20	0.0010	3.756e-05	0.0015	0.00144	5.384e-05
1/40	4.2565e-04	7.522e-06	6.2714e-04	5.9e-04	1.078e-05
1/80	1.7190e-04	1.517e-06	2.5377e-04	2.4e-04	2.173e-06
1/160	6.7826e-05	3.069e-07	1.0063e-04	9.5e-05	4.396e-07

TABLE 3.5: Comparison of L_2 errors and L_∞ error by proposed algorithm with the existing scheme for Ex. 3.6.1 at time $T = 1$, $\alpha = 0.7$, $h = 0.05$, $M = 4$ SLP basis.

x	PAE using SLP basis			PAE using SCP basis		
	$\alpha = 0.1$	$\alpha = 0.5$	$\alpha = 0.9$	$\alpha = 0.1$	$\alpha = 0.5$	$\alpha = 0.9$
0.0	3.495E-11	3.528E-09	1.240E-07	4.668E-11	5.067E-09	1.849E-07
0.1	1.638E-10	1.853E-08	5.964E-07	1.504E-10	1.704E-08	5.386E-07
0.2	3.521E-10	3.744E-08	1.228E-06	3.405E-10	3.623E-08	1.182E-06
0.3	5.175E-10	5.256E-08	1.744E-06	5.096E-10	5.174E-08	1.715E-06
0.4	6.471E-10	6.321E-08	2.118E-06	6.436E-10	6.282E-08	2.106E-06
0.5	7.283E-10	6.874E-08	2.324E-06	7.288E-10	6.870E-08	2.325E-06
0.6	7.485E-10	6.849E-08	2.333E-06	7.511E-10	6.862E-08	2.341E-06
0.7	6.949E-10	6.180E-08	2.119E-06	6.965E-10	6.183E-08	2.124E-06
0.8	5.549E-10	4.800E-08	1.657E-06	5.512E-10	4.756E-08	1.642E-06
0.9	3.159E-10	2.645E-08	9.179E-07	3.011E-10	2.507E-08	8.655E-07
1.0	3.495E-11	3.528E-09	1.240E-07	6.755E-11	6.409E-08	2.371E-07
L_2 error	5.308E-10	4.973E-08	1.682E-06	5.280E-10	4.937E-08	1.671E-06
L_∞ error	7.484E-10	6.873E-08	2.332E-06	7.511E-10	6.87E-08	2.341E-06
CPU time	14.99 sec.	14.82 sec.	14.91 sec.	89.42 sec.	89.00 sec.	92.28 sec.

TABLE 3.6: Point-wise absolute error (PAE) in x-direction and CPU time (in seconds) for Ex.3.6.1 with SLP and SCP basis at $T = 1$.

Now, we will discuss the case of non-homogeneous boundary condition.

Example 3.6.2. Consider the TFBSM (3.10) with initial condition $\mathcal{U}(x,0) = x^3 + x^2 + 1$, $(x,t) \in (0,1) \times (0,1)$, non-homogeneous boundary conditions $\mathcal{U}(0,t) = (t+1)^2$, $\mathcal{U}(1,t) = 3(t+1)^2$ and source function

$$f(x,t) = \left(\frac{2t^{2-\alpha}}{\Gamma(3-\alpha)} + \frac{2t^{1-\alpha}}{\Gamma(2-\alpha)}\right)(x^3+x^2+1) - (t+1)^2\left[a(6x+2) + b(3x^2+2x) - c(x^3+x^2+1)\right].$$

The exact solution of Ex. 3.6.2 is,

$$\mathcal{U}(x,t) = (t+1)^2(x^3+x^2+1). \tag{3.125}$$

Here, $\alpha = 0.7$, $\tau = 1/160$, $h = 0.05$, $M = 4$ SLP/SCP basis, $T = 1$, and the parameter values are $r = 0.5$, $\sigma = 0.25$, $a = \frac{1}{2}\sigma^2$, $a = 1$, $b = r - a$, $c = r$. The following outcomes of Ex. 3.6.2 are:

- Fig. 3.5 shows that at each time level, approximate solutions are in good agreement with the exact solutions in the case of non-homogeneous conditions also.
- Fig. 3.6 shows that the absolute error decreasing with the increase in time level. The effect of fractional order α to the solution profile is reflected in fig. 3.7. It can be observed that the absolute error is decreasing with a decrease in α.
- **Numerical stability:** The stability of our algorithm can be verified numerically by fig. 3.8. It shows the behavior of absolute errors in the absence of noise and in presence of two different noise in the initial condition, $\delta^1 = 0.1\%\mu^{100}$ and $\delta^2 = 10\sigma^{100}$. It is observed that the variation in the absolute error in

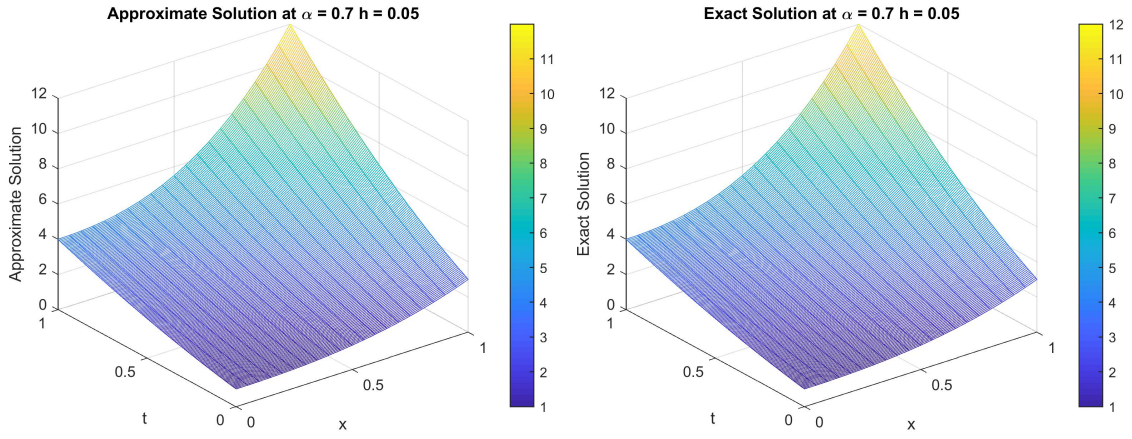

FIGURE 3.5: Surface plot of approximate solution (left) and exact solution (right) of Ex. 3.6.2 for $\alpha = 0.7$, $\tau = 1/160$ using $M = 4$ SLP basis

presence of noise is negligible as compared to without noise. This verifies the stability of our numerical algorithm in non-homogeneous case also.

- From Tables 3.7-3.10, we can say that L_2 and L_∞-errors are almost the same with both the basis function but the CPU time taken by the SLP basis is less than SCP basis. The temporal order of convergence (CO) with respect to L_2-norm and L_∞-norm is of order $(3-\alpha)$, which validates theoretical finding.

- A comparative study of L_2 and L_∞ errors, obtained by the proposed scheme and the scheme given in [1] and [2] is given in Table 3.11. It is observed from that the errors obtained by the proposed algorithm is much better than earlier study.

- Table 3.12 demonstrate the point wise absolute error (PAE) in spatial direction with respect to both the basis. It indicates that spatial accuracy also reaches from 10^{-8} to 10^{-10} for different values of α only using four number of basis functions. In this case also, the accuracy is almost uniform at each spatial grid point throughout the domain [0,1], for each α.

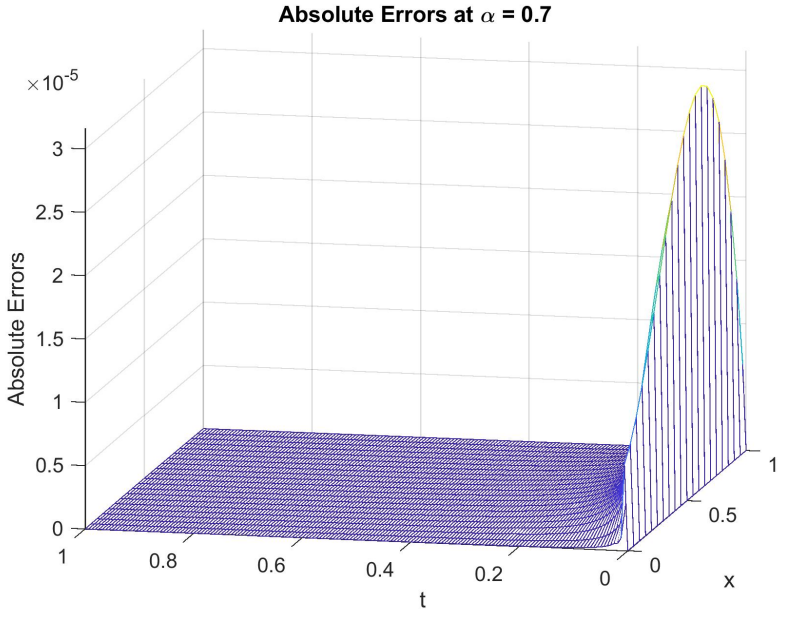

FIGURE 3.6: Absolute errors of Ex. 3.6.2 for $\alpha = 0.7$, $\tau = 1/160$ using $M = 4$ SLP basis.

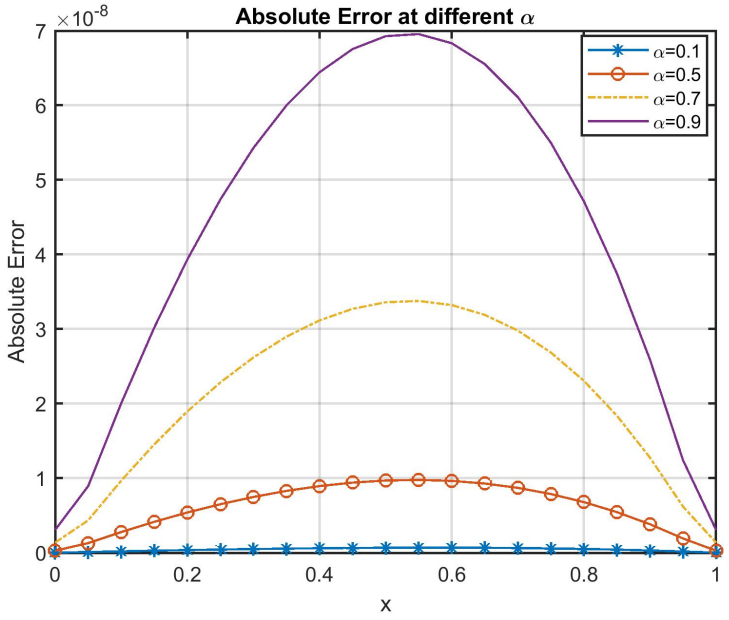

FIGURE 3.7: Absolute errors of Ex. 3.6.2 for different $\alpha = 0.7$ at $T = 1$ using $M = 4$ SLP basis.

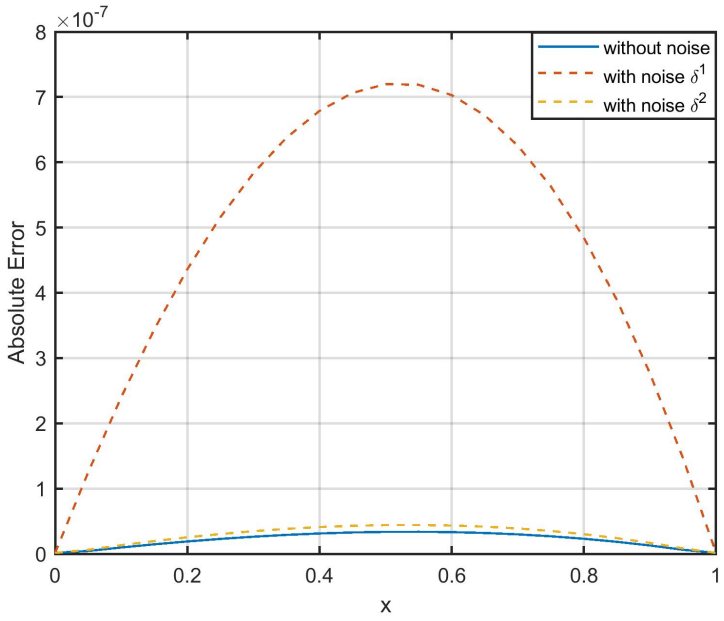

FIGURE 3.8: Absolute errors of Ex. 3.6.2 with different noise using $M = 4$ SLP basis.

τ	$\alpha = 0.1$			$\alpha = 0.5$			$\alpha = 0.9$		
	L_2 error	CO	CPU	L_2 error	CO	CPU	L_2 error	CO	CPU
1/10	2.074e-06	-	1.87	1.258e-05	-	1.96	1.978e-05	-	1.91
1/20	2.543e-07	3.028	3.19	1.809e-06	2.798	3.26	4.289e-06	2.205	3.23
1/40	3.166e-08	3.006	6.26	2.744e-07	2.721	6.35	9.498e-07	2.175	6.27
1/80	3.973e-09	2.995	11.89	4.331e-08	2.664	12.08	2.168e-07	2.132	11.86
1/160	5.005e-10	2.989	23.23	7.046e-09	2.620	23.32	5.014e-08	2.112	23.59

TABLE 3.7: L_2 error, order of convergence (CO) and CPU time (in seconds) for Ex. 3.6.2 using SLP basis at $T = 1$.

τ	$\alpha = 0.1$			$\alpha = 0.5$			$\alpha = 0.9$		
	L_∞ error	CO	CPU	L_∞ error	CO	CPU	L_∞ error	CO	CPU
1/10	2.838e-06	-	1.87	1.747e-05	-	1.96	2.780e-05	-	1.91
1/20	3.480e-07	3.028	3.19	2.519e-06	2.794	3.26	6.039e-06	2.203	3.23
1/40	4.333e-08	3.006	6.26	3.829e-07	2.718	6.35	1.338e-07	2.174	6.27
1/80	5.438e-09	2.994	11.89	6.057e-08	2.660	12.08	3.056e-07	2.131	11.86
1/160	6.852e-10	2.988	23.23	9.873e-09	2.617	23.32	7.069e-08	2.112	23.59

TABLE 3.8: L_∞ error, order of convergence (CO) and CPU time (in seconds) for Ex. 3.6.2 using SLP basis at $T = 1$.

τ	$\alpha = 0.1$			$\alpha = 0.5$			$\alpha = 0.9$		
	L_2 error	CO	CPU	L_2 error	CO	CPU	L_2 error	CO	CPU
1/10	2.076e-06	-	7.20	1.258e-05	-	7.25	1.973e-05	-	7.51
1/20	2.545e-07	3.028	12.85	1.808e-06	2.798	12.86	4.278e-06	2.205	12.86
1/40	3.169e-08	3.005	24.41	2.741e-07	2.721	24.46	9.474e-07	2.175	24.38
1/80	3.976e-09	2.994	49.56	4.326e-08	2.663	49.85	2.162e-07	2.131	49.56
1/160	5.009e-10	2.988	96.20	7.038e-09	2.619	96.58	5.001e-08	2.112	96.50

TABLE 3.9: L_2 error, order of convergence (CO) and CPU time (in seconds) for Ex. 3.6.2 using SCP basis at $T = 1$.

τ	$\alpha = 0.1$			$\alpha = 0.5$			$\alpha = 0.9$		
	L_∞ error	CO	CPU	L_∞ error	CO	CPU	L_∞ error	CO	CPU
1/10	2.856e-06	-	7.20	1.742e-05	-	7.25	2.747e-05	-	7.51
1/20	3.502e-07	3.027	12.85	2.508e-06	2.796	12.86	5.958e-06	2.205	12.86
1/40	4.361e-08	3.005	24.41	3.807e-07	2.719	24.46	1.319e-06	2.174	24.38
1/80	5.472e-09	2.995	49.56	6.013e-08	2.662	49.85	3.012e-07	2.132	49.56
1/160	6.896e-10	2.988	96.20	9.790e-09	2.618	96.58	6.968e-08	2.112	96.50

TABLE 3.10: L_∞ error, order of convergence (CO) and CPU time (in seconds) for Ex. 3.6.2 using SCP basis at $T = 1$.

τ	L_2 Error		L_∞ Error		
	[1]	Our Method	[1]	[2]	Our Method
1/10	0.0040	2.059e-05	0.0055	0.0052	2.882e-05
1/20	0.0016	3.516e-06	0.0022	0.00207	4.931e-06
1/40	6.5217e-04	6.445e-07	8.9427e-04	8.3e-04	9.056e-07
1/80	2.5638e-04	1.236e-07	3.5176e-04	3.3e-04	1.739e-07
1/160	9.5055e-05	2.434e-08	1.3065e-04	1.3e-04	3.426e-08

TABLE 3.11: Comparison of L_2 error and L_∞ error by proposed algorithm with existing scheme for Ex. 3.6.2 at time $T = 1$ when $\alpha = 0.7$, $h = 0.05$ and $M = 4$ SLP basis.

x	PAE using SLP basis			PAE using SCP basis		
	$\alpha = 0.1$	$\alpha = 0.5$	$\alpha = 0.9$	$\alpha = 0.1$	$\alpha = 0.5$	$\alpha = 0.9$
0.0	1.528E-11	2.849E-10	3.071E-09	2.085E-11	3.827E-10	4.190E-09
0.1	1.955E-10	2.785E-09	2.005E-08	1.991E-10	2.714E-09	1.925E-08
0.2	3.615E-10	5.404E-09	3.933E-08	3.634E-10	5.361E-09	3.884E-08
0.3	5.035E-10	7.487E-09	5.429E-08	5.041E-10	7.469E-09	5.407E-08
0.4	6.120E-10	8.947E-09	6.443E-08	6.116E-10	8.948E-09	6.442E-08
0.5	6.772E-10	9.695E-09	6.928E-08	6.763E-10	9.708E-09	6.938E-08
0.6	6.895E-10	9.644E-09	6.833E-08	6.886E-10	9.659E-09	6.844E-08
0.7	6.391E-10	8.708E-09	6.111E-08	6.390E-10	8.711E-09	6.109E-08
0.8	5.164E-10	6.800E-09	4.713E-08	5.177E-10	6.775E-09	4.682E-08
0.9	3.117E-10	3.831E-09	2.590E-08	3.153E-10	3.760E-09	2.511E-08
1.0	1.528E-11	2.849E-10	3.071E-09	2.210E-11	4.231E-10	4.536E-09
L_2 error	5.309E-10	7.048E-09	5.014E-08	5.009E-10	7.038E-09	5.001E-08
L_∞ error	7.485E-10	9.695E-09	6.928E-08	6.886E-10	9.708E-09	6.938E-08
CPU time	26.42	26.85	26.14	140.95	141.52	141.42

TABLE 3.12: Point-wise absolute error (PAE) in x-direction and CPU time (in seconds) for Ex.3.6.2 with SLP and SCP basis at $T = 1$.

Example 3.6.3. Consider the TFBSM (3.1) governing European double barrier knock-out call option with the barrier condition $\mathcal{C}(3,\zeta) = 0$, $\mathcal{C}(15,\zeta) = 0$, $(S,\tau) \in (3,15)\times(0,1)$ and terminal condition $\mathcal{C}(S,T) = \max(S-K,0)$. Here, the parameter values are $r = 0.03$, $\sigma = 0.45$, $T = 1$ (year), dividend yield $D = 0.01$ and the strike price $K = 10$. The solution has been performed by taking $M = 10$ elements of the SLP basis function for better approximation. The following outcomes of Ex. 3.6.3 are:

- It can also be observed from the fig.3.9 that when the stock price is greater than some critical value near the strike price K, the European double barrier call option price increases as α decreases as we see that the amplitude of the peak increase as α decreases.
- Since, the TFBSM reduces to classical B-S model when α=1 and from the fig.3.9 one can see that the option price $\mathcal{C}(S,T)$ for the TFBSM is lower than the option price for the classical BSE when $S < K$ and higher than classical B-S model when $S > K$. This indicates that the jump nature of the option pricing can be better reflected in the TFBSM as compared to the classic B-S model.

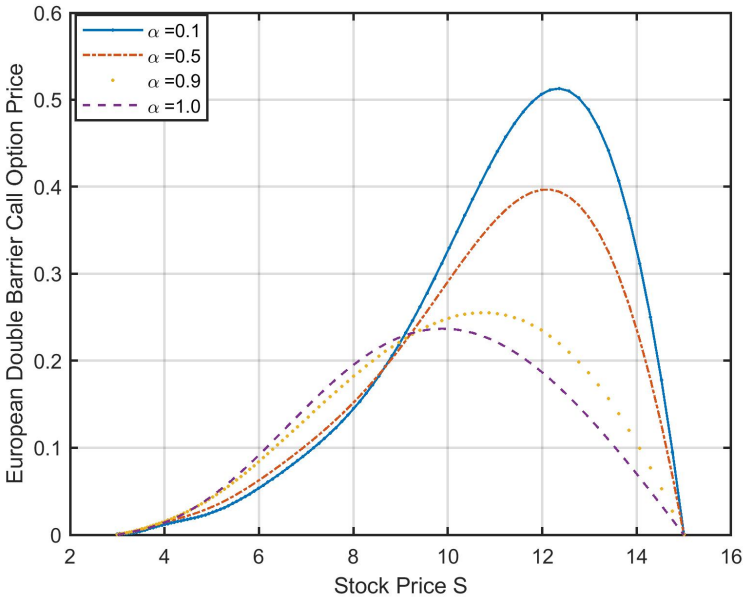

FIGURE 3.9: European double barrier option price for different α at $r = 0.03$, $\sigma = 0.45$, $T = 1$, $K = 10$, dt=0.0125 and $M = 10$ SLP basis.

3.6.3 The study of effects of different parameters on the European call/put option

In this section, we study the effect of various parameters like fractional order (α), volatility (σ), interest rate (r), strike price (K) on the option pricing.

Example 3.6.4. Consider the TFBSM (3.1) governing European call option with the barrier condition $\mathcal{C}(3,\zeta) = 0,\ \mathcal{C}(15,\zeta) = S - Ke^{-r(1-\zeta)},\ \ (S,\zeta) \in (3,15) \times (0,1)$ and terminal condition $\mathcal{C}(S,T) = \max(S-K,0)$. Here, dividend yield $D = 0$. We have taken $M = 10$ elements of the SLP basis function for the better approximation. The following outcomes of example 3.6.4 are:

- Fig.3.10 shows the approximate solution of European call option $\mathcal{C}(S,\zeta)$ for different value of $\alpha = 0.1, 0.5, 0.9$ when strike price $K = 10$, $r = 0.05$, $\sigma = 0.3$. It can be seen from the zoomed image that when the stock price 'S' is near the

strike price K, the European call option price increases as α increases. The order of the time-fractional derivative α influence the behavior of European call option profile.

- Fig. 3.11 shows the effect of volatility 'σ' on the stock price movement when $K = 10$, $r = 0.05$, $\sigma = 0.1, 0.2, 0.3, 0.4$, $\alpha = 0.5$. It can be observed that when the stock price S is near the strike price K, the higher the volatility is, the higher the option price. This confirms a popular saying in the real financial world, i.e., "High Risk, High Return".

- The effect of risk-free interest rate 'r' on the European call option price is shown in Fig. 3.12 for $K = 10$, $r = 0.005, 0.05, 0.1, 0.2$, $\sigma = 0.3$, $\alpha = 0.5$. This validates that higher the interest rate, higher the call option price will be.

- Fig. 3.13 talks about the effect of strike price 'K' on the European call option price for $r = 0.05$, $\sigma = 0.3$, $\alpha = 0.5$. It says that, when the strike price goes up, the European call option price goes down.

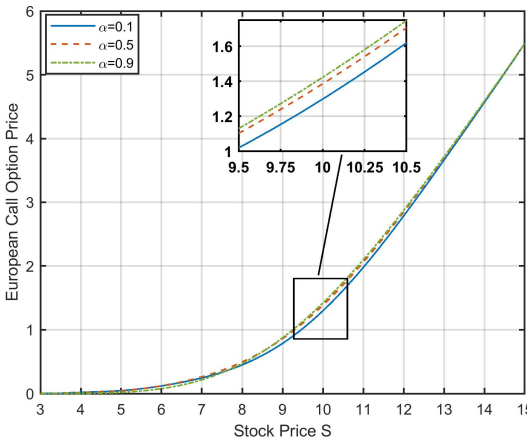

FIGURE 3.10: Effect of fractional order α in Ex. 3.6.4

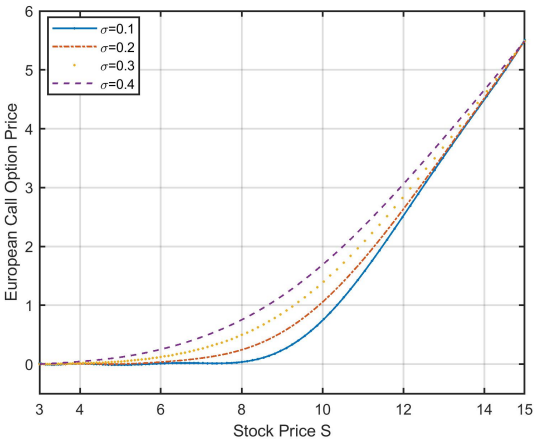

FIGURE 3.11: Effect of volatility σ in Ex. 3.6.4

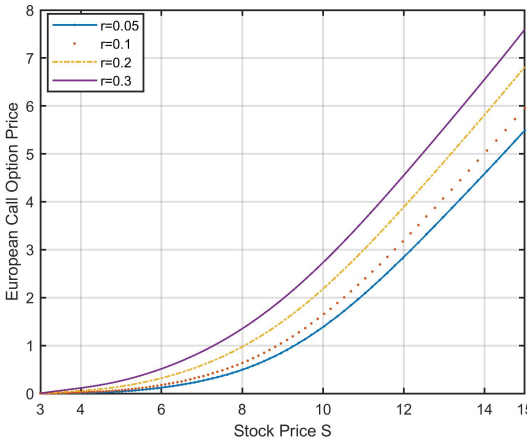

FIGURE 3.12: Effect of interest rate r in Ex. 3.6.4

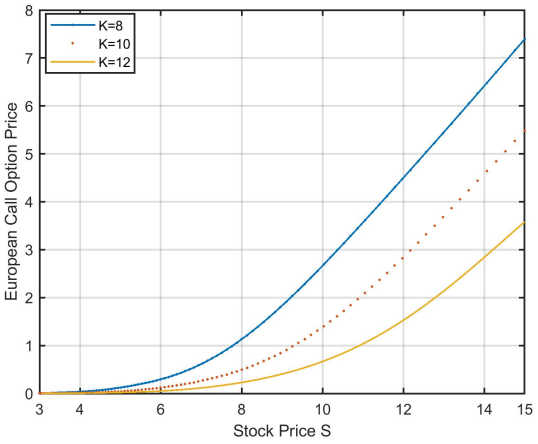

FIGURE 3.13: Effect of Strike price K in Ex. 3.6.4

Example 3.6.5. Consider the TFBSM (3.1) governing European put option with the barrier condition $\mathcal{C}(0.05,\zeta) = Ke^{-r(1-\zeta)}$, $\mathcal{C}(30,\zeta) = 0$, and terminal condition $\mathcal{C}(S,T) = \max(K-S,0)$. Here, dividend yield D=0. We have taken $M = 12$ elements of the SLP basis function for the better approximation. The following outcomes of example 3.6.5 are:

- Fig.3.14 shows the approximate solution of European put option $\mathcal{C}(S,\zeta)$ for different value of $\alpha = 0.1, 0.5, 0.9$ when strike price $K = 20$, $r = 0.05$, $\sigma = 0.3$.

It can be seen from the zoomed image that when the stock price 'S' is near the strike price K, the European put option price also increases a bit as α increases. Thus, we can say that order of the time-fractional derivative α influence the behavior of European put option profile.

- Fig.3.15 shows the effect of volatility 'σ' on the stock price movement when $K = 10$, $r = 0.05$, $\sigma = 0.2, 0.3, 0.4$, $\alpha = 0.5$. It can be observed that when the stock price S is near the strike price K, the higher the volatility is, the higher the option price. Thus, the phenomenon of "High Risk, High Return" is also true in the case of Europen put option price.

- The effect of risk-free interest rate 'r' on the European put option price is shown in Fig.3.16 for $K = 20$, $r = 0.05, 0.1, 0.2$, $\sigma = 0.3$, $\alpha = 0.5$. It can be seen that higher the interest rate, lower the put option price will be which is opposite case of European call option price.

- Fig.3.17 talks about the effect of strike price 'K' on the European put option price for $r = 0.05$, $\sigma = 0.3$, $\alpha = 0.5$. It says that, when the strike price goes up, the European put option price goes up too whereas the reverse happen in the case of European call option price.

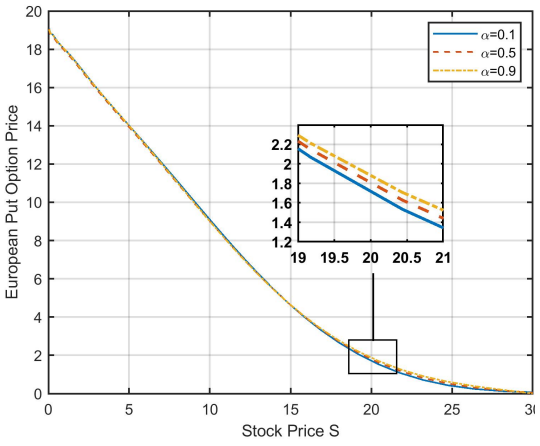

FIGURE 3.14: Effect of fractional order α in Ex. 3.6.5

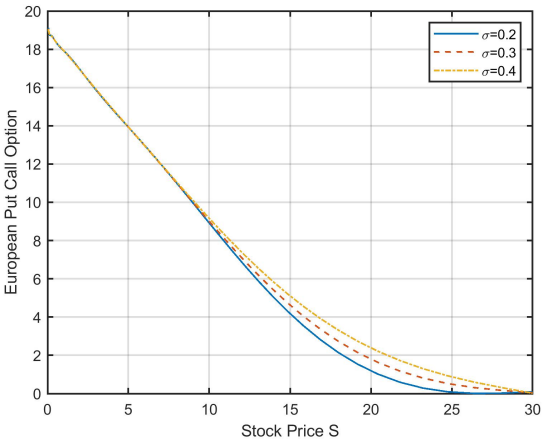

FIGURE 3.15: Effect of volatility σ in Ex. 3.6.5

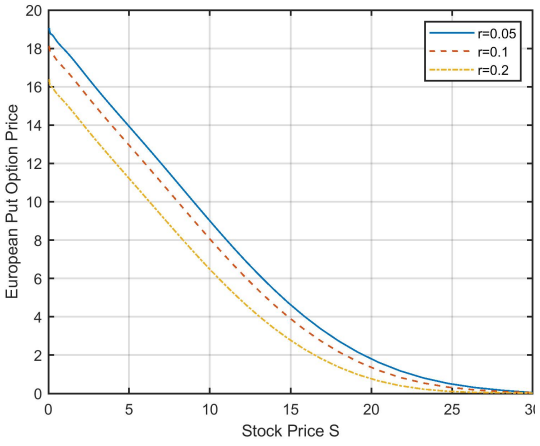

FIGURE 3.16: Effect of interest rate r in Ex. 3.6.5

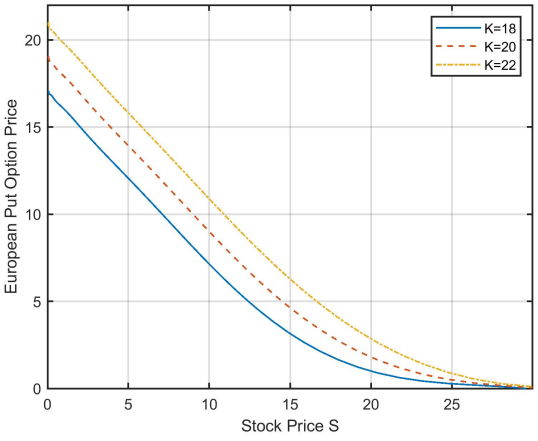

FIGURE 3.17: Effect of Strike price K in Ex. 3.6.5

3.7 Conclusion

In summary, we have designed a stable computational approach based on a combination of finite difference with an operational matrix approach for the TFBSM governing various European options. The algorithm is observed to be highly accurate and showing a higher order of convergence, (3-α) in time for all $\alpha \in (0, 1)$. It is observed from the Tables 3.1-3.12 that the L_2 and L_∞ error for Ex. 3.6.1 and Ex.

3.6.2 are almost same with both the basis functions but the CPU time taken by using SLP basis is less than the SCP basis function. The theoretical unconditional stability and convergence of the numerical scheme have been established for $\alpha \in (0, \bar{\alpha}]$ and a different approach is under investigation for $\alpha \in (\bar{\alpha}, 1)$. The stability and convergence of the scheme are also verified numerically. The comparative study of the numerical results with [1] and [2] are given in Table 3.5 and Table 3.11 have shown that the proposed algorithm perform better in terms of error efficiency and convergence order. The effect of fractional order α (see figs.3.10,3.14) and various other parameters like volatility (see figs.3.11,3.15), interest rate (see figs.3.12,3.16), and strike price (see figs.3.13,3.17) on the European call and put option pricing are also discussed in detail by using SLP basis function. These effects justify the physical phenomenon of the financial market. The proposed numerical algorithm is observed to be more error efficient and can be applied to various other time-fractional models, e.g., TFDE, TFADE, TFRDE, and TFBSM governing American options, which is one of our goal and a topic for future study.